DEVELOPMENT AND CHARACTERIZATION OF ION TRIGGERED *in-situ* NANOEMULGEL FOR INTRANASAL DELIVERY

Submitted by

SNEHANEEL MITRA

B. Pharm

EXAMINATION ROLL NO: **M4PHG24004**

REGISTRATION NO: **144399 of 2018-19**

Under the guidance of

Dr. MANAS BHOWMIK

Associate Professor

Division of Pharmaceutics

DEPARTMENT OF PHARMACEUTICAL TECHNOLOGY

Faculty of Engineering and Technology

JADAVPUR UNIVERSITY

Thesis submitted in partial fulfilment of the requirements for the

DEGREE OF MASTER OF PHARMACY

Department of Pharmaceutical Technology

Faculty of Engineering and Technology

JADAVPUR UNIVERSITY,

Kolkata-700032

Session: 2022-2024

CERTIFICATE OF APPROVAL

Department of Pharmaceutical Technology

Jadavpur University Kolkata - 700032

This is to certify that MR. SNEHANEEL MITRA, B. Pharm. (2018-22), has carried out the research work on the subject entitled "**DEVELOPMENT AND CHARACTERIZATION OF ION TRIGGERED *in-situ* NANOEMULGEL FOR INTRANASAL DELIVERY**" under my supervision of **Dr. MANAS BHOWMIK** in the Department of Pharmaceutical Technology of this university. He has incorporated his findings into this thesis of the same title, being submitted by him, in partial fulfilment of the requirements for the degree of Master of Pharmacy of Jadavpur University. He has carried out this research work independently and with proper care and attention to my satisfaction.

30/08/2024

Dr. MANAS BHOWMIK

Associate Professor,

Dept. Of Pharmaceutical

Technology Jadavpur University

Kolkata, 700032

Dr. Manas Bhowmik
Associate Professor
Dept. of Pharmaceutical Technology
Jadavpur University, Kol-700 032
West Bengal, India

30/8/24.

Prof. Dr. AMALESH SAMANTA

Head, Dept. Of Pharmaceutical

Technology Jadavpur University

Kolkata, 700032

Head
Dept. of Pharmaceutical Technology
Jadavpur University
Kolkata-700 032, W.B. India

Dipak Laha 30.8.24

Prof. DIPAK LAHA

Dean, Faculty of Engineering and

Technology, Jadavpur University

Kolkata, 700032

DEAN
Faculty of Engineering & Technology
JADAVPUR UNIVERSITY
KOLKATA-700 032

Declaration of Originality and Compliance of Academic Ethics

As a requirement for earning my Master of Pharmacy, I, SNEHANEEL MITRA officially certify that this thesis includes both original research and a survey of past research. This document contains all of the information that was gathered and presented in compliance with ethical standards and academic regulations.

I further declare that I have cited and referenced any materials and results that are not original to my work, as required by these rules and conduct.

Name: SNEHANEEL MITRA

Exam Roll Number: M4PHG24004
Class Roll Number: 002211402025
Registration Number: 144399 0f 2018-19

Thesis Title: "DEVELOPMENT AND CHARACTERIZATION OF ION TRIGGERED *in-situ* NANOEMULGEL FOR INTRANASAL DELIVERY"

Snehaneel Mitra
30/08/2024

SNEHANEEL MITRA

Signature with Date

ACKNOWLEDGEMENT

I would like to express my heartfelt gratitude to my guide **Dr. Manas Bhowmik** and co-guide **Prof. (Dr.) L. K. Ghosh**, Division of Pharmaceutics, Department of Pharmaceutical Technology, Jadavpur University, Kolkata, for their unwavering support, guidance, and mentorship throughout my journey as a Master's student in Pharmaceutics at Jadavpur University. Their expertise, dedication, constant encouragement and insightful feedback have been invaluable in shaping the research presented in this thesis.

I am also thankful to Dr. Dipankar Chattapadhyay (Department of Polymer Science and Technology, University of Calcutta) for providing some materials and their valuable suggestions.

This acknowledgement will be incomplete without the faculty members and head of the department, **Prof. Amalesh Samanta** of the Department of Pharmaceutical Technology, Jadavpur University for their valuable inputs, encouragement, and academic resources that have enriched my educational experience.

I extend my appreciation to the team of our Pharmaceutics Laboratory-II, research scholars Ekta Yadav, Riasree Paul, Ananya Ghosh, Gyamcho Bhutiya, seniors Saban Karmakar Rinchen Palzong Bhutia, Moumoyee Chakraborty and Bikram Roy, batchmates Sagar Roy Biswadeep Das, and Mahesh Kumar, juniors Prince Kumar, Debjoti Das, Subrata Maity and Abdul Ajij for their camaraderie, discussions, and shared passion for pharmaceutical research. Your collective efforts have made this academic pursuit both enjoyable and rewarding.

I express my thanks to UGC, Ministry of Human Resource and Development, Government of India, for providing the financial assistance in the form of AICTE GPAT PG fellowship.

A word of thanks to all those people associated with this work directly or indirectly whose names I have been unable to mention here. My parents for whom I do not not have enough words to express my thanks.

Lastly, I would like to thank myself. I want to thank myself for believing in me. I want to thank me for doing all the research, for all the hard work. I want to thank myself for not having to depend on anyone, working all by myself and having no days off. I want to thank myself for never quitting, no matter how miserable the times were. I want to thank myself for always being a giver and trying to give more than I receive. I want to thank myself for doing more right than wrong. I would especially thank me for not forgetting who I am and being just me.

CONTENTS

1. INTRODUCTION

1.1.THE BLOOD BRAIN BARRIER

The Central Nervous System (CNS) is a complex and sophisticated system that regulates and co-ordinates various body activities. It is vulnerable to various vascular structural and functional disorders **[1].** Thus, CNS disorders represent increasing social and economic problems all over the world due to high morbidity and mortality **[2].** Furthermore, many CNS diseases like Alzheimer's disease and Parkinson's disease need chronic therapies **[3].** Despite the immense network of the cerebral vasculature, systemic delivery of therapeutics to the CNS is not effective for greater than 98% of small molecules and for nearly 100% of large molecules **[8].**

Generally, low molecular weight compounds (<400 Da) which are lipophilic and non-ionisable at physiological pH can cross the blood-brain-barrier (BBB) through diffusion **[6]**. The BBB is a system of layers of cells at the cerebral capillary endothelium, the choroid plexus epithelium, and the arachnoid membranes, which are connected by tight junctions and which together separate the brain and the cerebrospinal fluid (CSF) from the blood **[10]**. These tight endothelial junctions can be 100 times tighter than junctions of other capillary endothelium **[11]**. Thus, the barrier has many properties similar to a continuous cell membrane, allowing lipid-soluble molecules to transport across the membrane where hydrophilic solutes demonstrate minimal permeation **[12]**.

While certain small molecule, peptide, and protein therapeutics given systemically reach the brain parenchyma by crossing the BBB **[6],** generally high systemic doses are needed to achieve therapeutic levels, which can lead to adverse effects in the body. Many strategies have been explored for effective drug delivery to the brain by vanquishing the challenges of BBB, both invasive and non-invasive **[4]**. BBB is highly restrictive in the access of molecules to the brain; it allows entry of only nutrients and mediators that are required to maintain brain homeostasis **[5]**.

Therapeutics can be introduced directly into the CNS by intracerebroventricular or intraparenchymal injections; however, for multiple dosing regimens both delivery methods are invasive, risky, and expensive techniques requiring surgical expertise and also slow diffusion from the injection site and rapid turnover of the cerebrospinal fluid (CSF) **[9].** Thus the invasive approaches are a non-preferred method of drug delivery to the brain due to various risks associated with the procedures **[7].**

1.2.DRUG DELIVERY TO BRAIN

The non-invasive route for delivery of drugs to CNS can be achieved via two pathways.

- **Delivery across the BBB** by either manipulation of the drug to make it permeable to BBB (prodrug approach) or by utilisation of carriers or transporters. However, these methods are complex and require drugs to possess certain specific characteristics and hence do not work effectively for all therapeutic agents. Drugs are administered by classical intravenous or intraperitoneal injections, or through the digestive tract, lung, or skin. However, part of these lipophilic chemicals are subject to being metabolised in the liver, resulting in a modification in the amount of circulating drug available to the brain. Moreover, the liver, kidney, intestine, skin, lung and also tissues separating the brain from the blood flow, express enzymes able to metabolise xenobiotics. Another part of the dosage may be excreted by the kidney before entry into the CNS, rendering the precise amount of the drug that finally enters the brain difficult to be estimated. Similarly, drug delivery by intracerebroventricular (ICV) devices (catheter, or osmotic pumps for intraventricular drug infusion) or by surgical implantation of devices that release an active molecule near its pharmacological target for variable time durations, has its own limitations.

- **Bypassing the BBB** by intranasal delivery provides a practical, non-invasive, rapid and simple method to deliver the therapeutic agents to the CNS. This method works because of the unique connection between the nose and the brain that has evolved to sense odours and other chemical stimuli. The intranasal route of administration is not a novel approach for drug delivery to the systemic circulation. The novelty lies in using this noninvasive method to rapidly deliver drugs directly from the nasal mucosa to the brain and spinal cord with the aim of treating CNS disorders while minimising systemic exposure.

The intranasal route of administration is easily amenable to self-administration and offers a non-invasive and virtually painless alternative to oral and parenteral administration for the delivery of drugs to the CNS **[13].** Intranasal delivery does not require any modification of the therapeutic agents and does not require that drugs be coupled with any carrier like in case of drug delivery across the BBB.

1.3.ADVANTAGES AND LIMITATIONS OF NASAL DELIVERY

1.3.1. Advantages of intranasal delivery:

- Non-invasive, rapid and comfortable
- Bypasses the BBB and targets the CNS, reducing systemic exposure and thus systemic side effects
- Does not require any modification of the therapeutic agent being delivered
- Works for a wide range of drugs. It facilitates the treatment of many neurologic and psychiatric disorders
- Rich vasculature and highly permeable structure of the nasal mucosa greatly enhance drug absorption
- Problem of degradation of peptide drugs is minimised up to a certain extent
- Easy accessibility to blood capillaries
- Avoids destruction in the gastrointestinal tract, hepatic "first pass" elimination and gut wall metabolism, allowing increased, reliable bioavailability.
-

1.3.2. Limitations to intranasal delivery:

- Concentration achievable in different regions of the brain and spinal cord, varies with each agent
- Delivery is expected to decrease with increasing molecular weight of drug
- Some therapeutic agents may be susceptible to partial degradation in the nasal mucosa or may cause irritation to the mucosa
- Nasal congestion due to cold or allergies may interfere with this method of delivery
- Frequent use of this route results in mucosal damage (e.g. infection, anosmia).

1.4.ANATOMY AND CELLULAR STRUCTURE OF THE NOSE

The nose is divided into two nasal cavities via the septum. The volume of each cavity is approximately 7.5 mL and has a surface area around 75 cm **[14]**. There are three different functional regions in the nose-vestibular, respiratory, and olfactory. Of these, the respiratory region is the most important for systemic drug delivery **[15]**. Figure 1 shows the cross-section of a human nose. The respiratory epithelium consists of basal, mucus-containing goblet, ciliated columnar and non-columnar cell types **[16].** The Celia moves in a wavelike fashion to transport particles from the pharynx area for ingestion **[17].** Additionally, the cells in this region are covered by 300 microvilli, providing a large surface area for absorption **[15].** Below the epithelium is lamina propria. This is the region where blood vessels, nerves, serous glands, and mucus secretory glands may be found **[16].** The lamina propria also houses a dense network of capillaries, many of which are very permeable for drug absorption **[20].**

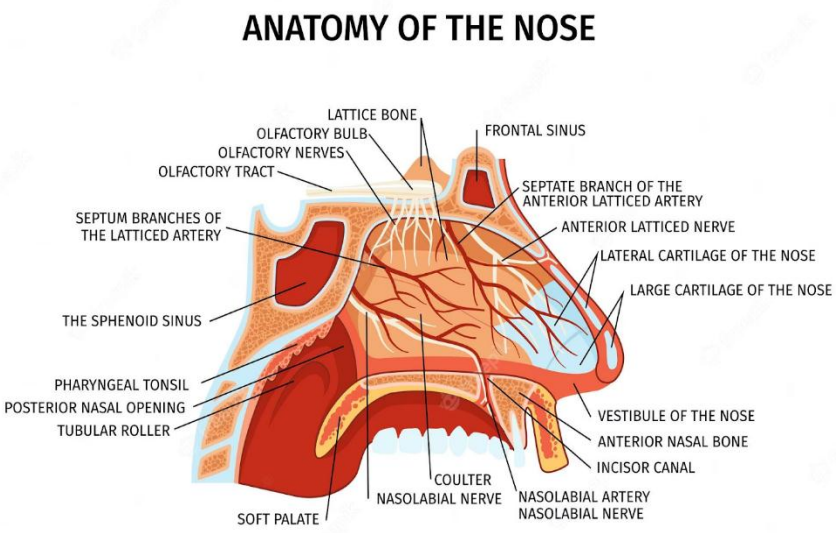

Figure 1.1: Anatomy of the Nose

The nasal epithelium is covered by a mucus layer that is renewed every 10 to 15 min.[18] The pH of mucosal secretion ranges from 5.5 to 6.5 in adults and from 5.0 to 6.5 in children **[19].** The mucus layer entraps particles, which are then cleared from the nasal cavity by the cilia. The rate of mucus flow through the nose is approximately 5 to 6 mm/min resulting in particle clearance within the nose every 20 min **[20].**

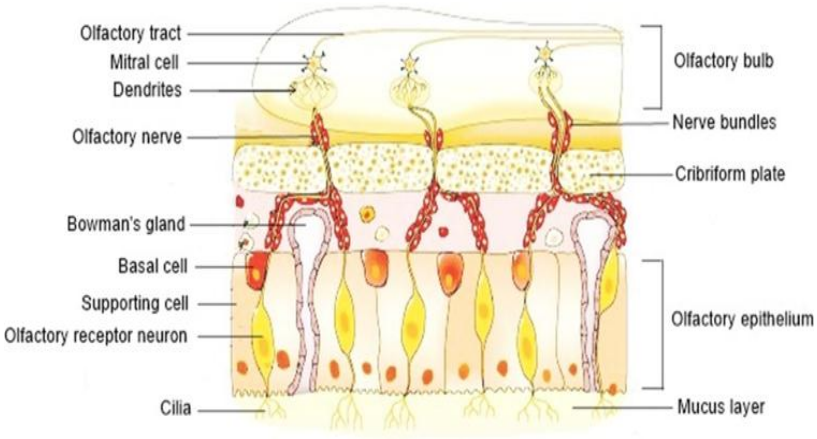

Figure 1.2: Cellular Structure of Nose

The olfactory nerves, which originate as specialised olfactory nerve endings (chemoreceptors) in the mucous membrane of the roof of the nasal cavity above the superior nasal conchae, are the sensory nerves of smell. On each side of the septum nerve fibres pass through the cribriform plate of the ethmoid bone of the olfactory bulb where interconnections and synapses occur. From the bulb, a bunch of nerve fibres pass through the olfactory tract and reach the olfactory area in the temporal lobe of the cerebral cortex in each hemisphere, where the impulses are interpreted and odour is perceived. Another set of nerves emanating from the nasal cavity is the maxillary branch of the trigeminal nerves, which are general sensory nerves **[21].**

1.5.TRANSPORT OF DRUGS FROM NASAL CAVITY

While the exact mechanisms underlying intranasal drug delivery to the CNS are not entirely understood, an accumulating body of evidence demonstrates that pathways involving nerves connecting the nasal passages to the brain and spinal cord are important. In addition, pathways involving the vasculature, cerebrospinal fluid, and lymphatic system have been implicated in the transport of molecules from the nasal cavity to the CNS. It is likely that a combination of these pathways is responsible, although one pathway may predominate, depending on the properties of the therapeutic, the characteristics of the formulation, and the delivery device used. Figure 3 shows the uptake of a drug from the nasal cavity.

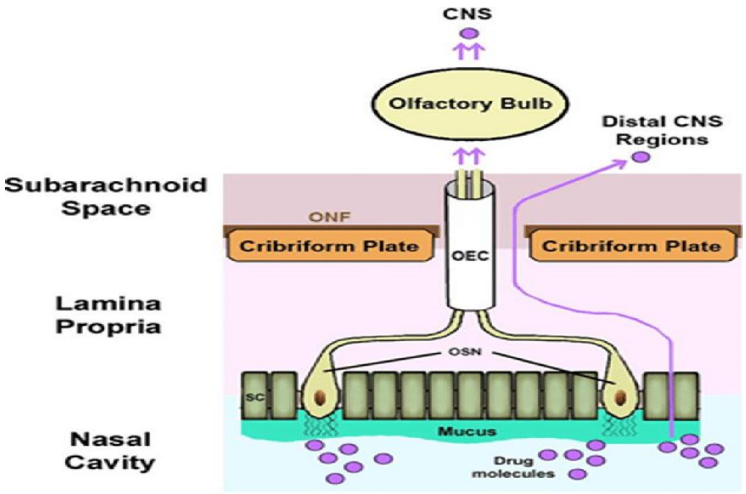

Figure 1.3: Drug Transport into the Brain

Two mechanisms are involved in the nasal delivery, a fast rate that depends on lipophilicity, and a slower rate that depends on molecular weight. Their absorption studies are consistent with the non-specific diffusion of the penetrant molecules through aqueous channels located between the nasal mucosal cells, which impose a size restriction on nasal permeability. Good bioavailability can be achieved for molecules up to 1000 Da (without enhancers) and can be extended to at least 6000 Da with the help of enhancers.

The transport mechanism for protein and amino acids involve absorption by an active saturable transport process, which appears to be Na+ dependent, and transport may require metabolic energy as a driving force.

Water-soluble substances are absorbed well and nasal absorption probably depends on aqueous channel diffusion (pores) **[22].** The molecular size of the molecule determines the rate of absorption in such channels.

1.6.THE NASAL ROUTE OF DELIVERY

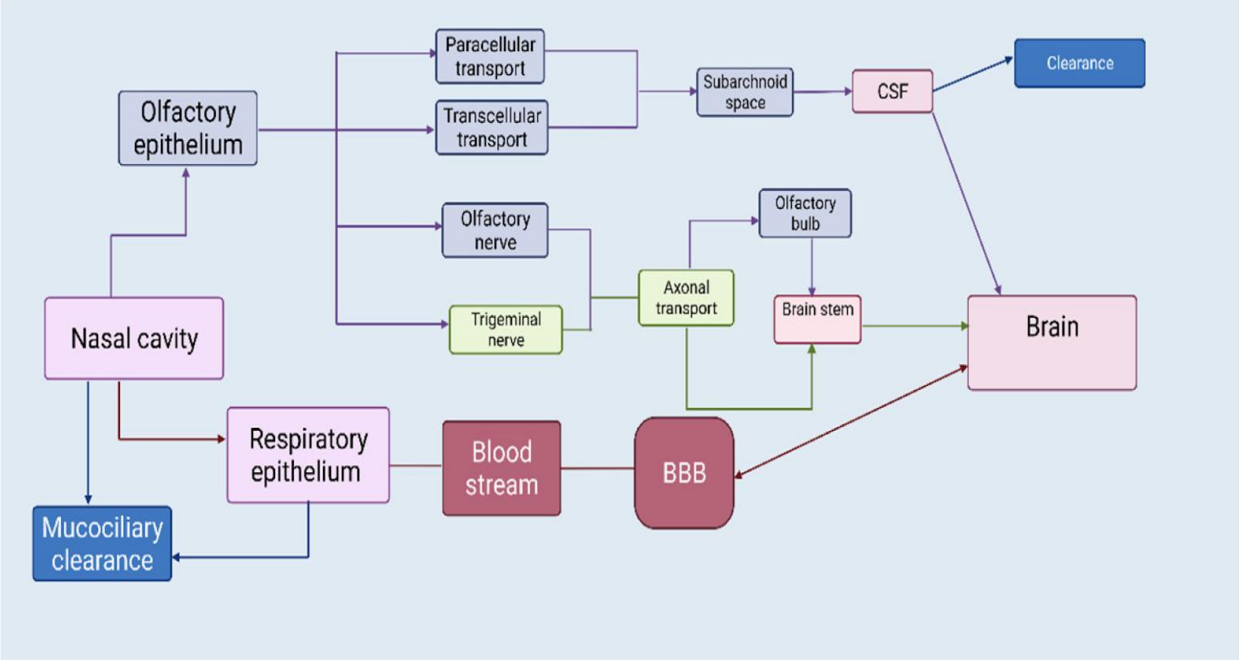

Figure 1.4: Nasal Delivery Pathways

1.6.1. Olfactory Nerve Pathway

Therapeutics can rapidly gain access to the CNS following intranasal administration along olfactory nerve pathways leading from the nasal cavity directly to the CNS. Olfactory nerve pathways are a major component of intranasal delivery, evidenced by the fact that fluorescent tracers are associated with olfactory nerves as they traverse the cribriform plate **[23]**, drug concentrations in the olfactory bulbs are generally among the highest CNS concentrations observed **[24] [25] [26]**, and a strong, positive correlation exists between concentrations in the olfactory epithelium and olfactory bulbs **[27]**.

Olfactory pathways arise in the upper portion of the nasal passages, in the olfactory region, where olfactory receptor neurons (ORNs) are interspersed among supporting cells , microvillar cells, and basal cells. ORNs mediate the sense of smell by conveying sensory information from the peripheral environment to the CNS **[28]**. Beneath the epithelium, the lamina propria contains mucus secreting Bowman's glands, axons, blood vessels, lymphatic vessels, and connective tissue. The dendrites of ORNs extend into the mucous layer of the olfactory

epithelium, while axons of these bipolar neurons extend centrally through the lamina propria and through perforations in the cribriform plate of the ethmoid bone, which separates the nasal and cranial cavities. The axons of ORNs pass through the subarachnoid space containing CSF and terminate on mitral cells in the olfactory bulbs. From there, neural projections extend to multiple brain regions including the olfactory tract, anterior olfactory nucleus, piriform cortex, amygdala, and hypothalamus **[29]**. In addition to ORNs, chemosensory neurons located at the anterior tip of the nasal cavity in the Grueneberg ganglion lead into the olfactory bulbs **[30] [31]**.

1.6.2. Trigeminal Nerve Pathway

The trigeminal nerve innervates the respiratory and olfactory epithelium of the nasal passages and enters the CNS via pons **[28] [32]**. The trigeminal nerve conveys sensory information from the nasal cavity, the oral cavity, the eyelids, and the cornea, to the CNS via the ophthalmic division (V1), the maxillary division (V2), or the mandibular division (V3) of the trigeminal nerve **[28] [32]**. The ophthalmic division of the trigeminal nerve branches provides innervation to the dorsal nasal mucosa and the anterior portion of the nose, while branches of the maxillary division provide innervation to the lateral walls of the nasal mucosa. The three branches of the trigeminal nerve come together at the trigeminal ganglion and extend centrally to enter the brain at the level of the pons, terminating in the spinal trigeminal nuclei in the brainstem.

A unique feature of the trigeminal nerve is that it enters the brain from the respiratory epithelium of the nasal passages at two sites:

- Through the anterior lacerated foramen near the pons
- Through the cribriform plate near the olfactory bulbs, creating entry points into both caudal and rostral brain areas following intranasal administration.

While there is not enough knowledge of ensheathing cells and channels associated with the trigeminal nerve comparable to those observed with the olfactory nerves, these anatomical features may be present along the trigeminal nerve. It is also likely that other nerves that innervate the face and head, such as the facial nerve, or other sensory structures in the nasal

cavity, such as the Grueneberg ganglion, may provide entry points for intranasally applied therapeutics into the CNS **[25]**.

1.6.3. Vascular Pathways

The nasal mucosa is highly vascular, receiving its blood supply from branches of the maxillary, ophthalmic and facial arteries, which arise from the carotid artery **[28]**. The olfactory mucosa receives blood from small branches of the ophthalmic artery, whereas the respiratory mucosa receives blood from a large calibre arterial branch of the maxillary artery.

Delivery to the CNS following absorption into the systemic circulation and subsequent transport across the BBB is possible, especially for small, lipophilic drugs, which more easily enter the bloodstream and cross the BBB compared to large, hydrophilic therapeutics such as peptides and proteins **[28]**. It is also possible that rather than being distributed throughout the systemic circulation, drugs can enter the venous blood supply in the nasal passages where they are rapidly transferred to the carotid arterial blood supply feeding the brain and spinal cord, a process known as countercurrent transfer **[33] [34] [35]**. However, delivery through the systemic circulation results in problems related to drug elimination via hepatic and renal mechanisms, and is limited by other factors including: the BBB, drug binding to plasma proteins, degradation by plasma proteases, and potential peripheral side effects.

1.6.4. CSF and Lymphatics Pathway

Pathways connecting the subarachnoid space containing CSF, perineurial spaces encompassing olfactory nerves, and the nasal lymphatics are important for CSF drainage and these same pathways provide access for intranasally applied therapeutics to the CSF and other areas of the CNS **[36] [37]**. Drugs can access the CNS via these same pathways after intranasal administration, moving from the nasal passages to the CSF to the brain interstitial spaces and perivascular spaces for distribution throughout the brain **[38]**.

1.7.REFERENCES

1. Demarquay, G., Ryvlin, P., & Royet, J. P. (2007). Olfaction et pathologies neurologiques: revue de la littérature. Revue Neurologique, 163(2), 155-167.

2. Feigin, V. L., Nichols, E., Alam, T., Bannick, M. S., Beghi, E., Blake, N., ... & Fischer, F. (2019). Global, regional, and national burden of neurological disorders, 1990–2016: a systematic analysis for the Global Burden of Disease Study 2016. The Lancet Neurology, 18(5), 459-480.

3. Borsook, D. (2012). Neurological diseases and pain. Brain, 135(2), 320-344.

4. Upadhyay, R. K. (2014). Drug delivery systems, CNS protection, and the blood brain barrier. BioMed research international, 2014.

5. Daneman, R., & Prat, A. (2015). The blood–brain barrier. Cold Spring Harbor perspectives in biology, 7(1), a020412.

6. Banks, W. A. (2009). Characteristics of compounds that cross the blood-brain barrier. BMC neurology, 9(Suppl 1), S3.

7. Dong, X. (2018). Current strategies for brain drug delivery. Theranostics, 8(6), 1481.

8. Pardridge WM. 2005. The blood-brain barrier: Bottleneck in brain drug development. NeuroRx 2:3–14.

9. Frey WH II. 2002. Bypassing the blood-brain barrier to deliver therapeutic agents to the brain and spinal cord. Drug Del Tech 2:46–49.

10. Oldendorf, W. (1976). Permeability Mechanisms: Blood-Brain Barrier in Physiology and Medicine. Stanley I. Rapoport. Raven, New York, 1976. xii, 316 pp., illus. $25. Science, 194(4264), 518-518.

11. Butt, A. M., Jones, H. C., & Abbott, N. J. (1990). Electrical resistance across the blood- brain barrier in anaesthetized rats: a developmental study. The Journal of physiology, 429(1), 47-62.

12. Neuwelt, E. A., Abbott, N. J., Drewes, L., Smith, Q. R., Couraud, P. O., Chiocca, E. A., ... & Doolittle, N. D. (1999). Cerebrovascular biology and the various neural barriers: challenges and future directions. Neurosurgery, 44(3), 604-608.

13. Keller, L. A., Merkel, O., & Popp, A. (2022). Intranasal drug delivery: Opportunities and toxicologic challenges during drug development. Drug delivery and translational research, 1-23.

14. Pomponi, M., Giacobini, E., & Brufani, M. (1990). Present state and future development of the therapy of Alzheimer disease. Aging Clinical and Experimental Research, 2, 125-153.

15. Illum, L. (2000). Transport of drugs from the nasal cavity to the central nervous system. European journal of pharmaceutical sciences, 11(1), 1-18.

16. Schipper, N. G., Verhoef, J. C., & Merkus, F. W. (1991). The nasal mucociliary clearance: relevance to nasal drug delivery. Pharmaceutical research, 8, 807-814.

17. Mathison, S., Nagilla, R., & Kompella, U. B. (1998). Nasal route for direct delivery of solutes to the central nervous system: fact or fiction?. Journal of drug targeting, 5(6), 415-441.

18. Chien, Y. W., & Chang, S. F. (1987). Intranasal drug delivery for systemic medications. Critical reviews in therapeutic drug carrier systems, 4(2), 67-194.

19. Hehar, S. S., Mason, J. D. T., Stephen, A. B., Washington, N., Jones, N. S., Jackson, S. J., & Bush, D. (1999). Twenty- four hour ambulatory nasal pH monitoring. Clinical Otolaryngology & Allied Sciences, 24(1), 24-25.

20. Mygind, N., & Änggård, A. (1984). Anatomy and physiology of the nose—pathophysiologic alterations in allergic rhinitis. Clinical reviews in allergy, 2, 173-188.

21. Waugh, A., & Grant, A. (2009). Anatomy and physiology in health and illness.

22. Fisher, A. N., Brown, K., Davis, S. S., Parr, G. D., & Smith, D. A. (1987). The effect of molecular size on the nasal absorption of water-soluble compounds in the albino rat. Journal of pharmacy and pharmacology, 39(5), 357-362.

23. Jansson B, Bjork E. 2002. Visualization of in vivo olfactory uptake and transfer using fluorescein dextran. J Drug Target 10:379–386.

24. Thorne RG, Pronk GJ, Padmanabhan V, Frey WH II. 2004. Delivery of insulin-like growth factor-I to the rat brain and spinal cord along olfactory and trigeminal pathways following intranasal administration. Neuroscience 127:481–496.

25. Banks WA, During MJ, Niehoff ML. 2004. Brain uptake of the glucagon-like peptide-1 antagonist exendin(9-39) after intranasal administration. J Pharmacol Exp Ther 309:469–475.

26. Ross TM, Martinez PM, Renner JC, Thorne RG, Hanson LR, Frey WH II. 2004. Intranasal administration of interferon beta bypasses the bloodbrain barrier to target the central nervous system and cervical lymph nodes: A non-invasive treatment strategy for multiple sclerosis. J Neuroimmunol 151:66–77.

27. Dhuria SV, Hanson LR, Frey WH II. 2009. Novel vasoconstrictor formulation to enhance intranasal targeting of neuropeptide therapeutics to the central nervous system. J Pharmacol Exp Ther 328: 312–320.

28. Clerico DM, To WC, Lanza DC. 2003. Anatomy of the human nasal passages. In: Doty RL, editor. Handbook of olfaction and gustation. 2nd edition. New York: Marcel Dekker, Inc. pp. 1–16.

29. Buck LB. 2000. The chemical senses. In: Kandel ER, Schwartz JH, Jessell TM, editors. Principles of neural science. 4th edition. New York: McGrawHill Companies. pp. 625–652.

30. Fuss SH, Omura M, Mombaerts P. 2005. The Grueneberg ganglion of the mouse projects axons to glomeruli in the olfactory bulb. Eur J Neurosci 22:2649–2654.

31. Koos DS, Fraser SE. 2005. The Grueneberg ganglion projects to the olfactory bulb. Neuroreport 16:1929–1932.

32. Gray H. 1978. Gray's anatomy. 15th revised edition (Classic Collectors edition). New York: Bounty Books.

33. Einer-Jensen N, Hunter R. 2005. Counter-current transfer in reproductive biology. Reproduction 129:9–18.

34. Einer-Jensen N, Larsen L. 2000. Transfer of tritiated water, tyrosine, and propanol from the nasal cavity to cranial arterial blood in rats. Exp Brain Res 130:216–220.

35. Stefanczyk-Krzymowska S, Krzymowski T, Grzegorzewski W, Wasowska B, Skipor J. 2000. Humoral pathway for local transfer of the priming pheromone androstenol from the nasal cavity to the brain and hypophysis in anaesthetized gilts. Exp Physiol 85: 801–809.

36. Bradbury MW, Cserr HF, Westrop RJ. 1981. Drainage of cerebral interstitial fluid into deep cervical lymph of the rabbit. Am J Physiol 240:F329–F336.

37. Bradbury MW, Westrop RJ. 1983. Factors influencing exit of substances from cerebrospinal fluid into deep cervical lymph of the rabbit. J Physiol 339:519–534.

38. Johnston M, Zakharov A, Papaiconomou C, Salmasi G, Armstrong D. 2004. Evidence of connections between cerebrospinal fluid and nasal lymphatic vessels in humans, non-human primates and other mammalian species. Cerebrospinal Fluid Res 1:2.

2. AIM AND OBJECTIVES

2.1.AIM

Delivery of Drugs to the CNS is a very challenging task due to the presence of BBB. The Nasal Route of Delivery bypasses the CNS and provides an easier alternative for Brain Targeting. Since, Lipophilic Drugs are easier to pass through the Brain, an *in-situ* nanoemulgel system was aimed to develop.

2.2.OBJECTIVES

- To check the solubility of drugs in various excipients.
- Screening of Oil, Surfactant and Co-surfactant.
- Preformulation study of the selected Drug and Excipients.
- Optimisation of the Developed Systems.
- Evaluation and Characterization of the Optimised systems
- *In-vitro* study of the final formulations.

3. LITERATURE REVIEW

Khan S. et al, 2020 developed a mucoadhesive temperature-mediated in situ gel formulation using chitosan and HPMC to enhance intranasal delivery of the dopamine D2 agonist ropinirole to the brain. Formulations were tested for gelation time, thermosensitivity, mucoadhesion, in vitro release and permeation, in vitro cytotoxicity, nasal clearance, in vivo bioavailability and brain uptake. In vivo bioavailability and brain uptake of ropinirole were assessed in albino wistar rats following intranasal administration of ropinirole in situ gel, intranasal ropinirole solution and I.V. ropinirole solution. Radiolabeled ropinirole uptake was calculated as a fraction of administered dose. The absolute bioavailability of ropinirole from the temperature-mediated in situ gelling nasal formulation was 82%. The AUC in the brain after nasal administration of ropinirole in situ gel was 8.5 times compared to I.V. administration, this value was also considerably higher than that achieved with intranasal ropinirole solution. High brain direct drug transport percentage (DTP) of 90.36% and drug targeting index (DTI) > 1 confirms direct nose to brain transport of the intranasal in situ gel formulation of ropinirole.

Mahdi M. H. et al, 2015 investigated high acyl gellan as a nasal drug delivery vehicle. High acyl gellan produces highly elastic gels below 60 °C which make it difficult to spray using a mechanical spray device. The problem was addressed by making fluid gels by introducing a shear force during gelation of the gellan polymer. These fluid gel systems contain gelled micro-particles suspended in a solution of un-gelled polymer. The systems therefore behaved as pourable viscoelastic fluids. Investigation of the rheological behaviour and mucoadhesion properties of fluid gels of two different types of gellan (high and low acyl) and fluid gels prepared from blends of high and low acyl gellan at a 50:50 ratio. The results demonstrated that by preparing fluid gels of high acyl gellan, the rheological properties were sufficient to spray through a standard nasal spray device. Moreover fluid gels also significantly enhance both high acyl and low acyl gellan mucoadhesion properties.

Salem H. F. et al, 2019 aimed at formulating a nasal nano-emulgel of resveratrol, using carbopol 934 and poloxamer 407 as the gelling agent. The optimum nano-emulsion was determined through further characterization of the selected system. The nasal nano-emulgel was prepared and tested for the in vitro release, the release kinetics, FTIR, ex vivo permeation, nasal mucosa toxicity and in vivo pharmacokinetic study. The optimum nano-emulsion

consisted of tween 20, capryol 90 and transcutol at a ratio of (54.26, 23.81 & 21.93 %v/v respectively), it exhibited transmittance of 100%, resveratrol solubility of 159.9±6.4 mg/ml, globule size of 30.65 nm. The in vitro resveratrol released from nano-emulsion and nasal nasal nano-emulgel was 96.17±4.43% and 78.53±4.7% respectively. Ex vivo permeation was sustained during 12 h up to 63.95±4.7%. The histopathological study demonstrated that the formula is safe and tolerable to the nasal mucosa. C_{max} and AUC of resveratrol obtained after nasal administration of nasal nano-emulgel was 2.23 and 8.05 times respectively. Similarly, Tmax was increased up to 3.67±0.82 h. The optimised nasal nano-emulgel established intranasal safety and bioavailability enhancement thus considering it as a well-designed system to target the brain.

Gadhave D. et al, 2023 designed a quetiapine hemifumarate (QF) loaded biodegradable nanoemulsion (QF-NE) with suitable surface charge modification by poloxamer-chitosan and evaluated its targeting efficiency against RPMI-2650 cell lines. QF-loaded poloxamer-chitosan in-situ gel (QF-Nanoemulgel) was formulated through the o/w emulsification aqueous titration technique and optimised using the QbD approach. Optimised QF-Nanoemulgel was evaluated for globule size of 15.0 ± 0.3 nm, PDI of 0.05 ± 0.001, Zeta Potential of − 18.3 ± 0.2 mV, %T of 99.8 ± 0.8 %, viscosity of 13.5 ± 2.1 cP, %EE of 69.0 ± 1.5 %, and ex-vivo mucoadhesive strength of 43.7 ± 1.5 g. QF-Nanoemulgel revealed sustained release and obeyed zero-order kinetics compared to QF-NE and QF-suspension. Nanoformulations treated blood samples did not cause hemolytic activity compared to drug and negative control after 10 h treatment. In-vitro cytotoxicity, cellular uptake, and permeation of 12.5 and 25 μM QF-Nanoemulgel were assessed on RPMI-2650 cells and discovered nontoxic with 0.55 ± 0.02 μg and 1.1 ± 0.04 μg cellular permeation, respectively, which ensured the safety and potency of QF-Nanogel.

Pires P. C. et al, 2019 developed thermosensitive nanoemulgels of phenytoin and fosphenytoin, in combination, for intranasal administration, with immediate and sustained release profiles. Nanoemulsions were prepared by adding the aqueous phase, containing gelling polymers in the case of nanoemulgels, to emulsion pre-concentrates, followed, in the optimised procedure, by premix membrane emulsification. Formulation design and optimization was guided by drug strength, rheological behaviour, osmolality, mean droplet size and PDI.

Fosphenytoin interferes significantly with Carbopol but not with Pluronic's gelation, and allowed to achieve drug strengths equivalent to 27 mg/g of phenytoin in lead nanoemulsions, and 16.7 mg/g of phenytoin in the lead nanoemulgel. The final selected low viscosity nanoemulsions had an immediate or prolonged fosphenytoin release profile, depending on anhydrous phase proportion (10% or 40%, respectively). The thermosensitive nanoemulgel, with 10% anhydrous phase, showed prolonged drug release.

Gadhave D. et al, 2023 fabricated amisulpride (AMS)-loaded intranasal in situ nanoemulgel (AMS-NG) in the treatment of schizophrenia. AMS nanoemulsion (AMS-NE) was prepared by employing aqueous-titration method and optimised using Box-Behnken statistical design. The optimised nanoemulsion was evaluated to obtain globule size of 92.15 nm, %Transmittance of 99.57%, Zeta Potential of −18.22 mV, and mucoadhesive strength of 8.90 g. The AMS-NE was converted to AMS-NG using poloxamer 407 and gellan gum. Following pharmacokinetic evaluation in Wistar rats, the brain Cmax for intranasal AMS-NG was found to be 1.48-folds and 3.39-folds higher when compared to intranasal AMS-NE and intravenous AMS-NE, respectively. Moreover, behavioural investigations of developed formulations were devoid of any extrapyramidal side effects in the experimental model. Finally, outcomes of the in vivo haematological study confirmed that intranasal administration of formulation for 28 days did not alter leukocytes and agranulocytes count. In conclusion, the promising results of Intranasal AMS-NG provided a novel platform for the effective and safe delivery of AMS in schizophrenic patients.

Mishra D. K. et al, 2013 improved sertraline hydrochloride (STH) solubility and formulated STH nanoemulsion (NE) for intranasal delivery to achieve rapid onset of action and to omit first pass effect with enhanced bioavailability. STH nanoemulsion (NE) system was formulated consisting of Capmul MCM as oil phase, tween 80 as surfactant and propylene glycol as cosurfactant. The developed system was characterised for phase behaviour and solubilization capacity and water titration method was utilised for the preparation of STH nanoemulsions (SNEs). All developed formulations were evaluated for globule size, drug content, nasal cilia toxicity, pH and viscosity. A high STH solubility of 94.28 mg/ml was observed with the NE system containing 20.0% Capmul MCM, 33.3% surfactant/co-surfactant (Labrasol:Transcutol

P at 2:1) and 46.7% water. In vitro diffusion studies for nasal absorption explanation were executed on goat nasal mucosa. In vitro nasal absorption through goat nasal mucosa was found to be 62.85±0.56%. These results suggested that intranasal delivery of STH to be beneficial compared to the available oral delivery for the treatment of depression.

Chin L. Y. et al, 2021 formulated telmisartan mucoadhesive nanoemulgel (TMNEG) for intranasal delivery. TMNEG was developed using Sefsol 218 and oleic acid (oil mix), Tween 20 (surfactant) and Transcutol P (co-surfactant), followed by incorporation of different concentrations of chitosan solution. The droplet-size, sizedistribution, zeta potential, pH and viscosity were evaluated for the developed TMNEG formulations. Later, mucoadhesive property, in vitro release pattern along with the mechanism of release and ex vivo permeation through goat nasal mucosa of the TMNEGs were evaluated. Photon correlation spectroscopy and thermodynamic stability studies had shown that optimised TMNEG formulation had a nanometric droplet size and acceptable pH. Drug release studies revealed that overall release in optimised TMNEG (57.45 ± 5.90%) is lower than optimised telmisartan nanoemulsion (71.71 ± 5.32%) within the time frame of 12 h, showing a delayed-release contributed by the chitosan coating. The higher release rate was found in both low and medium molecular weight chitosan-coated nanoemulgel at a concentration of 0.5% and 1.0% as compared to TMNEGs with high molecular weight chitosan. The in vitro release kinetic profile followed first-order reaction and Higuchi model with non-Fickian diffusion. Coating of nanoemulsion droplets with chitosan had shown to improve the mucoadhesive property, which further improved the permeation through goat nasal mucosa. Taking into consideration of mucoadhesive characteristics, extended drug release and improved ex vivo permeation, the developed TMNEG provides a potential platform for the delivery of telmisartan via intranasal route.

Nagaraja S. et al, 2021 designed a lipid-based nanoemulsifying drug delivery system of naringin using Acrysol K140 as an oil, Tween 80 as a surfactant and Transcutol HP as a cosolvent, to improve solubility and harness the benefits of nanosizing like improved cellular penetration. The naringin-loaded composition was optimised and characterised for various physicochemical and rheological properties. The formulation showed a mean droplet size 152.03 ± 4.6 nm with a PDI <0.23. Ex-vivo transmucosal permeation kinetics of the developed

formulation through sheep nasal mucosa showed sustained diffusion and enhanced steady-state flux and permeability coefficient. Scanning and transmission electron microscopy revealed the spherical shape of emulsion droplets and entrapment of droplets in a gel structure. The formulation showed excellent biocompatibility as analysed from the viability of L929 fibroblast cells and nasal mucosa histopathology after treatment. In vivo biodistribution studies revealed significantly higher drug transport and brain targeting efficiency.

Abdulla N. A. et al, 2021 developed nanoemulsion (NE) based in-situ gel of CZP for intranasal administration as an approach for bioavailability enhancement. Solubility of CZP was initially investigated in different oils, surfactants and co-surfactants, then pseudoternary phase diagrams were constructed to select the optimised ratio of oil, surfactant and co-surfactant. Clear and transparent NE formulations were characterised in terms of droplet size, viscosity, solubilization capacity, transmission electron microscopy, in-vitro drug release and compatibility studies. Selected NEs were incorporated into different in-situ gel bases using a combination of two thermosensitive polymers; Pluronic F-127 (PF127) and F-68 (PF68). NE-based gels (NG) were investigated for gelation temperature, viscosity, gel strength, spreadability and stability. Selected NGs were evaluated for ex-vivo permeation, mucoadhesive strength and nasal ciliotoxicity. Peppermint oil, tween 80 and transcutol P were chosen for NE preparation owing to their maximum CZP solubilization. Clear NE points extrapolated from tween 80:transcutol P (1:1) phase diagram and passed dispersibility and stability tests, demonstrated globule size of 67.99 to 354.96 nm and zeta potential of 12.4 to 3.11 mV with enhanced in-vitro CZP release (>90% in some formulations). After incorporation of the selected N3 and N9 formulations of Oil:Smix of 1:7 and 2:7, respectively to a mixture of PF127 and PF68 (20:2% w/w), the resultant NG formulations exhibited optimum gelation temperature and viscosity with enhanced CZP permeation and retention through sheep nasal mucosa. Ciliotoxicity examinations of the optimum NGs displayed no inflammation or damage of the lining epithelium and the underlying cells of the nasal mucosa.

Picco A. et al, 2023 studied in-vitro permeation through biomimetic membranes performed with Cannabigerol (CBG) and Cannabidiol (CBD) in the presence and in the absence of a randomly substituted methyl-β-cyclodextrin (MβCD). A new CBG extemporaneous emulgel (oil-in-gel emulsion) formulation was developed by spraydrying. The powder (SDE) can be

easily reconstituted with purified water, leading to a product with chemical-physical and technological characteristics that are comparable to those of the starting emulgels (E). Thermogravimetric analysis (TGA), attenuated total reflection-Fourier transformed infrared spectroscopy (ATR-FTIR), x-ray diffraction (XRD), and high-performance liquid chromatography (HPLC) analyses demonstrated that the spray-drying treatment did not alter the chemical properties of CBG. The work promised a metered-dosage form for the localised treatment of cutaneous afflictions such as acne and psoriasis.

Tungadi R. et al, 2020 characterised and evaluated nanoemulgel of snakehead fish powder (SFP) for the poorly water-soluble drug. SFP was formulated into nanoemulsion utilising the best comparison of surfactant, co-surfactant, and oil. Diverse nanoemulsion components (oil, surfactant, and co-surfactant) were chosen based on solvency and emulsification capacity. SFP 0.1% loaded nanoemulsion which was tested by stress-stability testing which carried out for all formulations and those that passed these tests were characterised for droplet size, polydispersity index (PDI), zeta potential, pH, viscosity, and transmittance. Later, the nanoemulsion was added with 1.5%, 2.0%, and 2.5% of HPMC in different concentrations and mixed until nanoemulgel form and evaluated for pH, viscosity, spreadability, and extrudability measurement. The results of this research showed that SF nanoemulsion produced a clear, stable, and transparent formula having the transmittance value 99.87%. Mean droplet size and zeta potential of the optimised nanoemulsion (NE4) were found to be 98.6±0.93 nm (PDI 0.1±0.20) and -57.5±0.3 MV respectively. The evaluation results of nanoemulgel (NEG) showed NEG1.5 gave pH 6.0, viscosity 210 cP, spreadability 5.8 g cm/s and extrudability 1.4 g/cm^2. NEG2.0 and NEG2.5 had high viscosity and pH generating low spreading on the skin i.e. 3.9 g cm/s and 2.8 g cm/s respectively. The results of the evaluation and preparation stability test showed a good level of stability of NEG 1.5 with the viscosity and pH by one way ANOVA which did not change significantly.

4. DRUG AND EXCIPIENT PROFILE

4.1.RESVERATROL

4.1.1. Introduction

Secondary metabolites are organic compounds produced by organisms that are not directly involved in their primary growth, development, or reproduction. Unlike primary metabolites, which include essential molecules like carbohydrates, proteins, and nucleic acids, secondary metabolites often serve various ecological functions such as defence mechanism, signalling, adaptation and competition.

Secondary Metabolites can be classified into various categories such as:

- Alkaloids: Nitrogen-containing alkaline compounds
- Terpenoids: Class of hydrocarbons derived from isoprene units
- Phenolics: Antioxidant compounds containing one or more phenol moiety
- Glycosides: A sugar moiety is bonded to a non-sugar moiety

Resveratrol (3,5,4'-trihydroxy-trans-stilbene) is a polyphenolic compound which was first identified in the roots of the white hellebore (*Veratrum grandiflorum*) in 1939 by Japanese chemist Michio Takaoka. Resveratrol has since been recognized as a key component in a range of plant-based foods, particularly grapes and red wine. The compound has a distinctive chemical structure comprising two phenolic rings connected by a trans-stilbene bridge, which is critical for its biological activity.

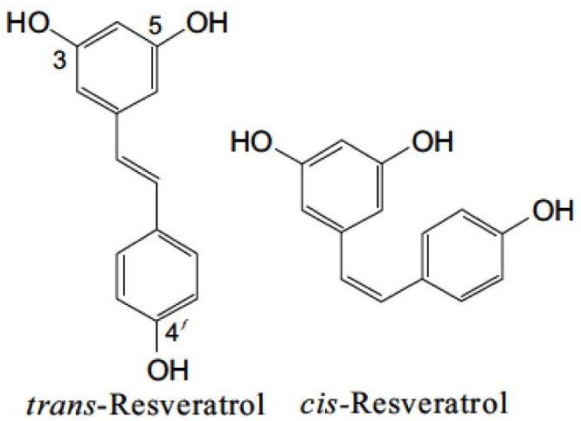

Figure 4.1.1 Chemical Structure of Resveratrol

The trans-stilbene configuration of resveratrol allows it to act as a potent antioxidant. Its hydroxyl groups at the 3, 5, and 4' positions play a significant role in its ability to neutralise reactive oxygen species (ROS) and chelate metal ions, thereby reducing oxidative stress and potential cellular damage **[5]**. This chemical structure contributes to resveratrol's wide array of biological effects, including anti-inflammatory, anticancer, and cardiovascular benefits.

4.1.2. Source

Resveratrol is found in various plant sources, with the most commonly being red wine and grapes. Other dietary sources include berries, such as blueberries and cranberries, and legumes like peanuts. The concentration of resveratrol varies significantly among these sources. 1 ml red wine typically contains about 0.01 to 0.03 mg of resveratrol, while grape skins and seeds can contain higher concentrations ranging from 0.1 to 1.5 mg per 100 grams **[6]**.

The bioavailability of resveratrol from dietary sources is relatively low due to its rapid metabolism and elimination from the body. After ingestion, resveratrol undergoes extensive metabolism in the gastrointestinal tract and liver, resulting in lower plasma concentrations than those found in the original food sources **[15]**. Despite this, resveratrol's presence in widely consumed foods and beverages continues to drive research into its health benefits.

4.1.3. Biological Activities

Antioxidant Activity

Resveratrol plays a crucial role in neutralising reactive oxygen species (ROS) and mitigating oxidative stress, which is linked to the pathogenesis of various chronic diseases (Rupasinghe et al., 2014). The primary mechanisms through which resveratrol exerts its antioxidant effects include:

Scavenging of ROS: Resveratrol has been shown to directly scavenge ROS such as superoxide radicals, hydrogen peroxide, and hydroxyl radicals. This scavenging activity helps reduce oxidative damage to cellular components, including lipids, proteins, and DNA (Rattan et al., 2004).

Activation of Antioxidant Enzymes: Resveratrol induces the expression of various antioxidant enzymes through the activation of transcription factors such as nuclear factor erythroid 2-related factor 2 (Nrf2). Nrf2 is a key regulator of the cellular antioxidant response and promotes the production of enzymes like glutathione peroxidase, superoxide dismutase, and catalase **[16]**.

Chelation of Metal Ions: Resveratrol can bind to metal ions such as iron and copper, which are known to catalyse the formation of ROS through Fenton and Haber-Weiss reactions. By chelating these metal ions, resveratrol reduces the generation of harmful ROS **[6]**.

Numerous studies have validated resveratrol's antioxidant properties. Research has demonstrated that resveratrol supplementation reduces oxidative stress markers in patients with metabolic syndrome and type 2 diabetes **[12]**. In experimental models, resveratrol has shown protective effects against oxidative damage in various tissues, including the liver, heart, and brain **[5]**.

Anti-inflammatory Effects

Resveratrol also exerts significant anti-inflammatory effects. It modulates several inflammatory pathways by various mechanisms:

Inhibition of NF-κB Activation: Resveratrol inhibits the activation of nuclear factor kappa B (NF-κB), a transcription factor that regulates the expression of pro-inflammatory cytokines such as tumour necrosis factor-alpha (TNF-α) and interleukins (IL-1β and IL-6). By suppressing NF-κB activation, resveratrol reduces inflammation and associated tissue damage **[1]**.

Modulation of COX and LOX Enzymes: Resveratrol inhibits the activity of cyclooxygenase (COX) and lipoxygenase (LOX) enzymes, which are involved in the production of pro-inflammatory prostaglandins and leukotrienes, respectively. This inhibition further contributes to its anti-inflammatory effects **[13]**.

Reduction of Nitric Oxide Production: Resveratrol reduces the production of nitric oxide (NO) by inhibiting the enzyme inducible nitric oxide synthase (iNOS). Elevated levels of NO are associated with inflammatory responses and tissue damage **[14]**.

In animal models, resveratrol has been shown to alleviate symptoms of inflammatory diseases such as rheumatoid arthritis and inflammatory bowel disease **[11]**. Clinical trials have also reported improvements in inflammatory markers and symptoms in patients with conditions like metabolic syndrome and cardiovascular disease **[8]**.

Cardiovascular Benefits

Improvement of Endothelial Function: Resveratrol enhances endothelial function by increasing the bioavailability of nitric oxide (NO). NO is a key regulator of vascular tone and

blood flow. By promoting NO production, resveratrol helps to maintain vascular health and reduce the risk of hypertension **[14]**.

Reduction of Platelet Aggregation: Resveratrol inhibits platelet aggregation and thrombosis, reducing the risk of clot formation and associated cardiovascular events. This effect is mediated through the modulation of platelet function and the inhibition of platelet activation pathways (Seyed et al., 2016).

Anti-atherogenic Effects: Resveratrol has been shown to inhibit the formation of atherosclerotic plaques by reducing oxidative modification of low-density lipoprotein (LDL) and inhibiting inflammatory responses in the arterial wall **[10]**.

The cardiovascular benefits of resveratrol have been supported by various studies. For instance, clinical trials have demonstrated that resveratrol supplementation can improve endothelial function and reduce blood pressure in patients with hypertension **[9]**. Additionally, experimental studies have shown that resveratrol reduces the progression of atherosclerosis and improves overall cardiovascular health **[15]**.

Anticancer Properties

Induction of Apoptosis: Resveratrol induces apoptosis in cancer cells by activating intrinsic and extrinsic apoptotic pathways. It enhances the expression of pro-apoptotic proteins like Bax and inhibits anti-apoptotic proteins like Bcl-2 **[7]**.

Inhibition of Tumour Growth: Resveratrol inhibits tumour growth by interfering with cell cycle progression and reducing cellular proliferation. It affects various cell cycle regulators, including cyclins and cyclin-dependent kinases (CDKs), thereby inducing cell cycle arrest **[8]**.

Prevention of Metastasis: Resveratrol inhibits metastasis by modulating processes such as epithelial-mesenchymal transition (EMT) and matrix metalloproteinase (MMP) activity. These processes are crucial for cancer cell invasion and metastasis **[7]**. The anticancer effects of resveratrol have been demonstrated in various cancer models, including breast, prostate, and colon cancers **[5]**. Resveratrol is potential as an adjunct to conventional cancer therapies, with promise in reducing tumour growth and improving patient outcomes **[15]**.

Neuroprotection

Neuroprotective effects of resveratrol have been explored in the context of neurodegenerative diseases such as Alzheimer's and Parkinson's disease. Resveratrol's neuroprotective effects are attributed to its ability to combat oxidative stress, reduce neuroinflammation, and enhance mitochondrial function:

Reduction of Oxidative Stress: Resveratrol reduces oxidative stress in the brain by scavenging ROS and enhancing the antioxidant defence system. This protection helps prevent neuronal damage and neurodegenerative diseases **[5]**.

Modulation of Neuroinflammation: Resveratrol inhibits neuroinflammatory responses by suppressing the activation of microglia and astrocytes. It also reduces the production of pro-inflammatory cytokines and inhibits the NF-κB signalling pathway **[1]**.

Enhancement of Mitochondrial Function: Resveratrol improves mitochondrial function by promoting mitochondrial biogenesis and reducing mitochondrial damage. This effect is mediated through the activation of sirtuins and the PGC-1α pathway **[3]**.

The neuroprotective effects of resveratrol have been demonstrated in various experimental models of neurodegenerative diseases, including Alzheimer's and Parkinson's diseases **[5]**. Clinical studies have also reported cognitive benefits and improvements in neurological function in patients receiving resveratrol supplementation **[2]**.

Studies have demonstrated that resveratrol can protect against cognitive decline and neuronal damage associated with these diseases **[5]**. However, further research is needed to fully elucidate its efficacy and mechanisms of action in neuroprotection.

4.1.4. Mechanism of Action

Sirtuin Activation

Sirtuins are a family of NAD+-dependent deacetylases that play a crucial role in regulating cellular processes such as ageing, metabolism, and stress response. Seven known sirtuins (SIRT1 to SIRT7) are present in the body. Activation of SIRT1 can improve metabolic health

and reduce inflammation, supporting its potential as a therapeutic agent for conditions like type 2 diabetes and cardiovascular disease **[1],[8]**. Activation of SIRT1 by resveratrol enhances deacetylation of target proteins, leading to various beneficial outcomes:

Metabolic Regulation: SIRT1 regulates metabolism by promoting fat oxidation and improving insulin sensitivity. It influences the expression of genes involved in metabolic processes, such as peroxisome proliferator-activated receptor gamma coactivator-1 alpha (PGC-1α), which is crucial for mitochondrial biogenesis and function **[4]**.

Anti-inflammatory Effects: SIRT1 inhibits the nuclear factor kappa B (NF-κB) signalling pathway, a key regulator of inflammation. By deacetylating and suppressing NF-κB, SIRT1 reduces the production of pro-inflammatory cytokines **[1]**.

Longevity and Aging: Through its effects on various cellular pathways, including stress resistance and DNA repair, SIRT1 contributes to increased lifespan and delayed onset of age-related diseases **[4]**.

AMP-Activated Protein Kinase (AMPK) Activation

AMPK is an energy-sensing enzyme that regulates cellular energy homeostasis. It is activated in response to low cellular energy levels, leading to a reduction in energy-consuming processes and an increase in energy-producing processes. Resveratrol activates AMPK, which mediates several key effects:

Metabolic Effects: Activation of AMPK by resveratrol enhances glucose uptake and fatty acid oxidation, contributing to improved insulin sensitivity and metabolic health **[3]**.

Mitochondrial Biogenesis: AMPK activation stimulates mitochondrial biogenesis through the PGC-1α pathway, enhancing mitochondrial function and energy production **[3]**.

Reduction of Inflammation: AMPK activation also inhibits inflammation by suppressing pro-inflammatory pathways, such as NF-κB **[3]**.

Oestrogen receptors (ERs) are nuclear hormone receptors that mediate the effects of oestrogen. There are two main types: ERα and ERβ. Resveratrol can interact with these receptors and

influence oestrogen-related processes. Resveratrol exhibits selective oestrogen receptor modulator (SERM) activity. It can bind to ERs and influence various oestrogen-dependent processes:

Bone Health: By modulating ERs, resveratrol has been shown to have beneficial effects on bone density and health, potentially reducing the risk of osteoporosis **[5]**.

Cancer Prevention: Resveratrol's interaction with oestrogen receptors is also relevant in the context of hormone-dependent cancers, such as breast cancer. It has been shown to inhibit the proliferation of oestrogen-dependent cancer cells **[7]**.

Autophagy Regulation

Autophagy is a cellular process that involves the degradation and recycling of damaged or dysfunctional cellular components. It is crucial for maintaining cellular homeostasis and function. Resveratrol regulates autophagy through several mechanisms:

Activation of SIRT1: By activating SIRT1, resveratrol promotes autophagy, as SIRT1 is known to enhance autophagic processes **[4]**.

Induction of Autophagy-related Genes: Resveratrol induces the expression of genes involved in autophagy, such as LC3 and Beclin-1, contributing to the removal of damaged cellular components and improving cellular health **[2]**.

Mitochondrial Function Enhancement

Mitochondria are the powerhouses of the cell, responsible for generating ATP through oxidative phosphorylation. Proper mitochondrial function is essential for energy production and cellular health. Resveratrol enhances mitochondrial function through multiple mechanisms:

Activation of PGC-1α: Resveratrol activates PGC-1α, a key regulator of mitochondrial biogenesis. This activation leads to an increase in mitochondrial number and function **[3]**.

Reduction of Mitochondrial Damage: Resveratrol also reduces oxidative damage to mitochondria, thereby protecting against mitochondrial dysfunction and associated diseases **[5]**.

Inhibition of Protein Kinases

Resveratrol inhibits various protein kinases, such as cyclin-dependent kinases (CDKs) and mitogen-activated protein kinases (MAPKs), which are involved in cell cycle regulation and cancer progression **[7]**.

Regulation of Apoptotic Pathways

Resveratrol influences apoptotic pathways by modulating pro-apoptotic and anti-apoptotic proteins, leading to the induction of apoptosis in cancer cells and protection of normal cells from excessive cell death **[7]**.

Modulation of Hormonal Pathways

Resveratrol interacts with several hormonal pathways, including insulin signalling, which contributes to its effects on metabolic health and diabetes **[6]**.

4.2.CAPRYOL 90

4.2.1. Chemical Structure

It is chemically known as Propylene Glycol MonoCaprylate composing of caprylic acid esterified with propylene glycol. Its chemical formula is $C_{12}H_{24}O_4$. The molecule consists:

- **Caprylic Acid:** An eight-carbon fatty acid with medium-chain length.
- **Propylene Glycol:** A diol with two hydroxyl groups, which provides the base for esterification.

4.2.2. Physical Properties

- **Appearance:** Capryol 90 is a clear, colourless to pale yellow liquid.
- **Odour:** It has a mild, characteristic odour.
- **Density:** Approximately 0.95 g/cm³ at 20°C.
- **Viscosity:** It has a low viscosity, which facilitates its use in various formulations.
- **Solubility:** Slightly soluble in water, soluble in organic solvents and miscible with other fatty acids and esters.
- **HLB value:** The compound has an HLB value of 6 making it a water-in oil surfactant.

4.2.3. Pharmaceutical Applications

Solubilization of Drugs

Capryol 90 is widely used in pharmaceutical formulations to enhance the solubility of lipophilic (fat-loving) drugs. Many active pharmaceutical ingredients (APIs) are poorly soluble in water but are soluble in organic solvents. Capryol 90 helps in creating stable solutions or suspensions of these APIs, thus improving their bioavailability and therapeutic efficacy **[17]**.

Emulsification

In the pharmaceutical industry, Capryol 90 acts as an emulsifier to stabilise emulsions, where oil and water phases are combined. This property is crucial in the formulation of creams, lotions, and other semi-solid formulations that require a stable mixture of hydrophobic and hydrophilic components **[18]**.

Enhancement of Drug Stability

Capryol 90 also contributes to the stability of pharmaceutical formulations by preventing the separation of drug components and maintaining uniformity throughout the product's shelf life. This is particularly important for formulations that are sensitive to environmental conditions like temperature and humidity **[19]**.

4.2.4. Cosmetic Applications

Solubilizer for Active Ingredients

In cosmetics, Capryol 90 is utilised to solubilize various active ingredients such as essential oils, vitamins, and other lipophilic substances. This ensures that these ingredients are evenly distributed throughout the cosmetic product, enhancing their effectiveness and stability **[20]**.

Skin Conditioning

Capryol 90 imparts a smooth, non-greasy feel to cosmetic products, which improves their texture and application. It is commonly found in creams, lotions, and serums, where it helps in spreading the product evenly and enhances the sensory attributes **[21]**.

Emulsification in Cosmetics

Capryol 90 serves as an effective emulsifier in cosmetic formulations, helping to stabilise emulsions and prevent phase separation. This property is essential in maintaining the consistency and quality of products like emulsions and gels **[22]**.

4.2.5. Food Industry

Flavour and Fragrance Carrier

In the food industry, Capryol 90 is used as a carrier for flavours and fragrances. Its solubilizing properties ensure that these volatile compounds are evenly distributed throughout food products, enhancing their sensory qualities **[23]**.

Emulsifier in Food Products

Capryol 90 also functions as an emulsifier in various food products, helping to stabilise emulsions such as dressings, sauces, and spreads. This application is important for achieving the desired texture and consistency in food formulations **[24]**.

4.3.ORYNOPHOR PH50

Chemically known as PEG-50 Hydrogenated Castor Oil. It is a derivative of castor oil, which consists primarily of ricinoleic acid, a fatty acid with a hydroxyl group. In the modification process, castor oil is first hydrogenated to saturate its fatty acids, reducing the number of double bonds. The hydrogenated castor oil is then reacted with polyethylene glycol (PEG) to produce the final product.

4.3.1. Chemical Structure

The compound is composed of three moieties:

- **Castor Oil**: Castor oil is composed of triglycerides, mainly ricinoleic acid (approximately 90%). Its structure includes a hydroxyl group on the 12th carbon of the fatty acid chain.
- **Hydrogenation**: This process saturates the double bonds in the fatty acids, converting unsaturated bonds to single bonds and increasing the stability of the oil.
- **Ethoxylation**: Involves the addition of ethylene oxide (EO) to the hydrogenated castor oil. PEG 50 indicates the average number of ethylene oxide units added, resulting in a polymer with a specific molecular weight and hydrophilic-lipophilic balance (HLB).

4.3.2. Chemical Formula

The precise formula can be complex due to variations in the number of PEG units and the degree of hydrogenation. Generally, Orynophor PH50 can be represented as:

$R-(OCH_2CH_2)_n-OH$

Where R represents the hydrogenated castor oil moiety and n indicates the average number of ethylene glycol units **[25]**.

4.3.3. Physical Properties

- **Appearance:** Pale yellow to transparent liquid at room temperature **[26]**.

- **Odour:** The compound generally has a mild or neutral odour, making it suitable for use in products where a strong scent is undesirable **[27]**.
- **Solubility:** soluble in water due to its PEG content, which imparts hydrophilic properties to the compound. Also soluble in a variety of organic solvents. This solubility enhances its utility and broadens its application for use in different formulations **[28]**.
- **HLB value:** The compound has an HLB value of 15.5 making it an oil-in-water surfactant.

4.3.4. Applications in Pharmaceutical Industry

Drug Delivery Systems

In pharmaceuticals, Orynophor PH50 is used to improve the solubility and stability of poorly soluble drugs. Its solubilizing and emulsifying properties facilitate the formulation of oral, topical, and injectable drug delivery systems **[29]**.

Topical Formulations

It is used in ointments and creams to improve the spreadability and absorption of active pharmaceutical ingredients **[30]**.

4.3.5. Applications in Cosmetics

Emulsifier

Orynophor PH50 is widely used as an emulsifier in creams, lotions, and gels. Its ability to stabilise oil-in-water and water-in-oil emulsions makes it valuable in cosmetic formulations **[31]**.

Solubilizer

It helps to dissolve lipophilic active ingredients into aqueous formulations, enhancing the efficacy of products such as shampoos and body washes **[32]**.

Conditioner

In hair care products, it acts as a conditioning agent, providing softness and manageability to the hair **[33]**.

Stabiliser

It helps stabilise formulations by preventing the separation of ingredients, ensuring uniform consistency in products such as sunscreens and moisturisers **[34]**.

4.4.DEGMEE

4.4.1. Chemical Structure

Diethylene Glycol Monoethyl Ether has the following chemical structure:

The structure features two ethylene glycol units linked by an ether bond with an ethyl group attached to one of the glycol units. This structure can be broken down into **[35]**:

- **Ethylene Glycol Units:** Two ethylene glycol groups (HO-CH_2 -CH_2 -OH)
- **Ether Linkage**: An oxygen atom connecting two ethylene glycol units
- **Ethyl Group:** An ethyl group (CH_3 -CH_2 -) attached to one of the glycol units

4.4.2. Physical Properties

- **Appearance:** Colourless, clear liquid with a mild, slightly sweet odour.
- **Boiling Point:** Approximately 207°C
- **Melting Point:** Approximately -68°C
- **Density:** About 1.08 g/cm³ at 20°C
- **Viscosity:** Relatively low, facilitating its use as a solvent and carrier
- **Solubility:** miscible with water, ethanol, and many organic solvents **[36]**.
- **pH**: Neutral in water

4.4.3. Pharmaceutical Applications

Solvent for Drug Formulations

DEGMEE is utilised as a solvent in various pharmaceutical formulations, including oral, topical, and injectable drugs **[17]**.

- **Oral Formulations**: DEGMEE is used to dissolve active pharmaceutical ingredients (APIs) in oral solutions and suspensions. Its solubility characteristics facilitate the effective delivery of APIs.

- **Topical Formulations**: In topical products, DEGMEE helps in solubilizing and stabilising active ingredients, contributing to product efficacy and stability.
- **Injectable Formulations**: DEGMEE is employed in injectable drug formulations, where it acts as a solvent for both APIs and excipients.

Excipients in Drug Delivery

In addition to serving as a solvent, DEGMEE is used as an excipient in drug delivery systems. It can enhance the solubility and bioavailability of poorly soluble drugs **[19]**.

- **Enhancing Bioavailability**: DEGMEE aids in the dissolution of hydrophobic drugs, improving their absorption and therapeutic efficacy.
- **Controlled Release Formulations**: DEGMEE is utilised in controlled release formulations, where it helps in the gradual release of the drug over time.

4.4.4. Cosmetic and Personal Care Applications

Solvent in Cosmetic Formulations

DEGMEE is employed in various cosmetic products due to its ability to dissolve and stabilise active ingredients **[21]**.

- **Skin Care Products:** In skin care formulations, DEGMEE helps in solubilizing ingredients such as vitamins and antioxidants, enhancing product efficacy and stability.
- **Hair Care Products:** DEGMEE is used in hair care products to improve the solubility of conditioning agents and other functional ingredients.

Emulsifier and Stabiliser

DEGMEE functions as an emulsifier and stabiliser in various personal care products, aiding in the formation and maintenance of emulsions **[22]**.

- **Emulsions:** DEGMEE helps in stabilising emulsions in creams and lotions, preventing phase separation and ensuring consistent texture.
- **Stability:** As a stabiliser, DEGMEE contributes to the long-term stability of cosmetic formulations, maintaining product performance and safety.

4.4.5. Applications in Food Industry

Solvent for Flavor and Fragrance Compounds

DEGMEE is employed as a solvent for certain flavour and fragrance compounds used in food and beverage products. Its ability to dissolve a range of substances makes it valuable in formulating flavours that need to be evenly distributed throughout a product **[37]**.

- **Flavouring Agents:** DEGMEE helps in dissolving and stabilising flavour compounds, ensuring that they are uniformly distributed and that their taste is consistent.
- **Fragrance:** In food and beverage products where aroma is crucial, DEGMEE serves as a carrier for fragrance ingredients, aiding in their incorporation into the final product.

Carrier Fluid in Food Colorants

In the formulation of food colourants, DEGMEE can act as a carrier fluid, aiding in the uniform dispersion of colourants in various food products **[38]**.

- **Colourant Formulations:** DEGMEE helps in dissolving pigments and dyes used in food products, ensuring even colouring and preventing clumping or separation.

Extraction Processes

DEGMEE can be used in extraction processes within the food industry, particularly in the extraction of specific compounds from natural sources **[39]**.

- **Essential Oils:** DEGMEE may be used in the extraction of essential oils and other valuable compounds from plant materials, contributing to the formulation of various food products.
- **Nutrient Extraction:** It can also assist in the extraction of nutrients and bioactive compounds, facilitating their incorporation into food products.

Food Processing

DEGMEE is used in food processing to stabilise emulsions, which are mixtures of oil and water **[40]**.

- **Emulsion Stabilisation:** DEGMEE helps maintain the stability of emulsions in dressings, sauces, and other food products by preventing phase separation and improving texture.

Plasticizers in Food Packaging

DEGMEE is sometimes used as a plasticizer in the production of food packaging materials. Its presence in packaging helps improve the flexibility and durability of films and containers **[41]**.

- **Packaging Materials:** DEGMEE contributes to the formation of flexible and durable plastic films used in food packaging, enhancing the protection and shelf-life of packaged foods.

4.5.GELLAN GUM

4.5.1. Introduction

Polysaccharide hydrogels are three-dimensional networks formed by the crosslinking of polysaccharides, which are long chains of carbohydrate molecules. These hydrogels are characterised by their ability to absorb and retain large amounts of water, making them useful in a variety of applications ranging from medical to food industries.

Gellan gum is a linear polysaccharide produced by the bacterium *Pseudomonas elodea*. It was Discovered in 1978 when scientists accidentally discovered bacteria growing in a pond in Pennsylvania, USA which produced a jelly-like substance on the base of lily pads. It has been available commercially since the early 1980s. The interest developed as it was highly thermoresistant and could produce gels of similar texture at very low concentrations. It was approved for use in food by USFDA in 1992. It was introduced to the food market as a substitute gelling agent for other stabilisers, like agar agar or gelatin.

4.5.2. Composition and Molecular Structure

Gellan gum is a high-molecular-weight polysaccharide produced by the bacterium *Sphingomonas elodea*. Its basic chemical structure consists of a tetrasaccharide repeating unit composed of:

- **D-Glucose:** β-D-glucopyranose units linked by β-1,4-glycosidic bonds.
- **L-Rhamnose:** α-L-rhamnopyranose units linked by α-1,3-glycosidic bonds.
- **D-Glucuronic Acid:** β-D-glucuronic acid units linked by β-1,4-glycosidic bonds.

The repeating tetrasaccharide unit is arranged in a linear chain, forming the backbone of gellan gum. The molecular formula is approximately $C_{41}H_{62}O_{32}$, with a molecular weight ranging from 10^4 to 10^6 Da, depending on the degree of polymerization **[42]**.

4.5.3. Gelation Properties

Thermoreversible Gels

High Acyl Gellan gum contains significant amounts of acetyl and glycerate ester groups. They form softer gels that can melt upon heating and solidify again upon cooling. This property is due to the reversible nature of the double-helical structures formed during gelation. Low Acyl Gellan gum contains fewer acyl groups and forms firm gels that do not revert to a sol state upon heating. These gels maintain their structure under various conditions The level of acylation affects the gel's texture, melting point, and rheological properties **[43] [44]**.

Ionic Gelation

The interaction of gellan gum with ions is crucial for its gel formation. Divalent cations like calcium ions are essential for gel formation in both HA and LA gellan gum. They facilitate the formation of the gel network by interacting with the carboxyl groups in gellan gum. Monovalent ions like sodium and potassium ions also form gels but they have less impact on gel formation as compared to calcium ions. The concentration of ions influences the strength and rigidity of the gel. Higher ion concentrations generally lead to stronger gels **[45]**.

pH of Gelling Solution

The pH of the solution also affects gellan gum’s solubility and gelation properties At lower pH values, gellan gum's gelation can be hindered due to the protonation of carboxyl groups, reducing the interaction with calcium ions thus forming weak gels. Gellan gum gelates more effectively in neutral to slightly alkaline conditions where the carboxyl groups are deprotonated, facilitating gel formation **[46]**.

4.5.4. Pharmaceutical Applications

Controlled Release Systems

Gellan gum is utilised in pharmaceutical formulations to achieve controlled drug release:

- **Matrix Tablets:** Gellan gum is used to create a matrix in sustained-release tablets, where its gel-forming properties help regulate the release of active pharmaceutical ingredients over time **[47]**.
- **Hydrogels:** Gellan gum-based hydrogels are used in drug delivery systems for their ability to swell and release drugs in a controlled manner **[48]**.

Wound Healing

In wound care, gellan gum's properties are leveraged to create effective wound dressings:

- **Moisture-Retentive Dressings:** Gellan gum-based hydrogels provide a moist environment that promotes wound healing and reduces pain during dressing changes **[49]**.

4.5.5. Cosmetic Industry

Thickener and Stabiliser

In cosmetics, gellan gum is valued for its thickening and stabilising effects:

- **Creams and Lotions:** Gellan gum is used to adjust the viscosity and stability of creams and lotions, enhancing their texture and application properties **[50]**.
- **Gels:** It is utilised in the formulation of clear gels, where its ability to form transparent, stable gels is advantageous **[51]**.

Encapsulation

Gellan gum’s encapsulation capabilities are also used in cosmetics to protect and deliver active ingredients:

- **Active Ingredient Delivery:** Gellan gum encapsulates active ingredients, such as vitamins and essential oils, ensuring their stability and controlled release **[52]**.

4.5.6. Medical and Biotechnological Applications

Tissue Engineering

Gellan gum's biocompatibility and gel-forming properties make it suitable for tissue engineering applications:

- **Scaffolds:** Gellan gum-based hydrogels are used to create scaffolds for tissue regeneration, providing a supportive matrix for cell growth and tissue development **[48]**.

Drug Delivery Systems

Gellan gum is employed in advanced drug delivery systems due to its controlled release characteristics:

- **Injectable Hydrogels:** Used for the development of injectable hydrogels that can deliver drugs or cells to specific sites in the body **[47]**.

Biotechnology

In biotechnology, gellan gum's properties are used for various purposes:

- **Cell Culture:** Gellan gum is used in cell culture applications as a substrate for growing cells, providing a stable and controlled environment **[45]**.
- **Water Purification:** Its ability to form gels can be utilised in water purification processes to remove contaminants **[42]**.

4.5.7. Applications in Food Industry

Gelling Agent

Gellan gum is widely used as a gelling agent in the food industry due to its ability to form gels with varying textures depending on its acylation and the presence of ions.

- **High Acyl Gellan Gum:** Used to prepare soft, elastic gels such as jellies, confectioneries, and dessert gels. These can be melted and reformed without loss of quality **[44]**.

- **Low Acyl Gellan Gum:** This type is used in products such as high-quality jams, jellies, and fruit preserves where a stable gel structure is crucial **[53]**.

Texture and Viscosity Enhancer

Gellan gum's thickening and stabilising properties are harnessed to improve the texture and consistency of various food products:

- **Beverages:** It helps in stabilising beverages like fruit drinks and dairy products by preventing sedimentation and ensuring uniform consistency **[45]**.
- **Sauces and Dressings:** Used to maintain the desired viscosity and texture of sauces and dressings, ensuring a smooth and appealing product **[51]**.

4.6.REFERENCES

1. Baur, J. A., & Sinclair, D. A. (2006). Therapeutic potential of resveratrol: The in vivo evidence. *Nature Reviews Drug Discovery*, 5(6), 493-506. doi:10.1038/nrd2060

2. Cascella, M., De Angelis, L., & Di Napoli, L. (2020). Resveratrol: Pharmacology and clinical applications. *Biomedicines*, 8(8), 293. doi:10.3390/biomedicines8080293

3. Hardie, D. G. (2014). AMPK: A target for drugs and natural products with effects on both diabetes and cancer. *Diabetes*, 63(11), 2767-2772. doi:10.2337/db14-0304

4. Lagouge, M., Argmann, C., & Gerhart-Hines, Z. (2006). Resveratrol improves mitochondrial function and protects against metabolic disease by activating SIRT1 and PGC-1α. *Cell*, 127(6), 1109-1122. doi:10.1016/j.cell.2006.11.013

5. Miller, A. A., & Park, J. H. (2011). Resveratrol and neuroprotection: A review of the mechanisms of action. *Frontiers in Aging Neuroscience*, 3, 30. doi:10.3389/fnagi.2011.00030

6. Pervaiz, S., & Holme, A. L. (2009). Resveratrol: Its biologic targets and functional activity. *Antioxidants & Redox Signaling*, 11(11), 2851-2897. doi:10.1089/ars.2009.2707

7. Salehi, B., Fokou, P. V. T., & Zucca, P. (2018). Resveratrol as an anticancer agent: A review of the molecular mechanisms. *Phytotherapy Research*, 32(10), 1924-1936. doi:10.1002/ptr.6103

8. Zang, J., Lu, X., & Qiu, H. (2020). Resveratrol modulates metabolic syndrome and diabetes through multiple mechanisms: A review. *Frontiers in Physiology*, 11, 349. doi:10.3389/fphys.2020.00349

9. Agewall, S., Cider, A., & Schenck-Gustafsson, K. (2012). Resveratrol for the prevention of cardiovascular events: A meta-analysis of randomized controlled trials. *JAMA*, 308(2), 135-145. doi:10.1001/jama.2012.7737

10. Giacomini, J., et al. (2010). Resveratrol content of grapes, grape-derived products, and wines. *Journal of Agricultural and Food Chemistry*, 58(15), 8230-8234. doi:10.1021/jf101425x

11. Kang, K. A., Piao, M. J., & Kim, K. C. (2012). Resveratrol and its analogs: Potential chemopreventive and chemotherapeutic agents. *Journal of Cellular Biochemistry*, 113(6), 1588-1597. doi:10.1002/jcb.24016

12. Poudyal, H., Panchal, S. K., & Brown, L. (2011). Resveratrol supplementation ameliorates oxidative stress and inflammation in type 2 diabetic rats. *Nutrition & Metabolism*, 8, 20. doi:10.1186/1743-7075-8-20

13. Schempp, C. M., Schuler, P., & Popp, S. (2004). Resveratrol and its effects on skin aging. *Phytomedicine*, 11(5), 409-414. doi:10.1078/0944711041465186

14. Vigna, G. B., Bencini, L., & Campi, R. (2013). Resveratrol inhibits platelet aggregation and thrombus formation. *Journal of Thrombosis and Haemostasis*, 11(9), 1526-1534. doi:10.1111/jth.12217

15. Wang, Y., Li, L., & Liu, Z. (2014). Resveratrol and cardiovascular disease: A review of clinical and experimental studies. *Journal of Cardiovascular Medicine*, 15(8), 551-558. doi:10.2459/JCM.0000000000000074

16. Zhang, Y., Lee, J. H., & Zhang, L. (2011). Resveratrol protects against oxidative stress in human cells and enhances antioxidant defenses. *Journal of Nutritional Biochemistry*, 22(4), 359-365. doi:10.1016/j.jnutbio.2010.01.012

17. Zhang, Y., Wang, X., & Wang, J. (2018). *Solubilization and stabilization of poorly soluble drugs in pharmaceutical formulations*. *International Journal of Pharmaceutics*, 550(1-2), 15-27. doi:10.1016/j.ijpharm.2018.07.011

18. Kothari, S., & Ghosh, S. (2019). *Role of emulsifiers in the pharmaceutical industry*. *Journal of Pharmaceutical Sciences and Research*, 11(5), 1695-1704. doi:10.5530/jpsr.2019.11.36

19. Fekete, S., & Horváth, S. (2018). *Stability of pharmaceutical formulations: Techniques and considerations*. *Pharmaceutical Research*, 35(1), 10. doi:10.1007/s11095-017-2327-5

20. Draelos, Z. D. (2016). *Cosmetic dermatology: Products and procedures*. *Wiley-Blackwell*. doi:10.1002/9781118773581

21. Farris, P. K. (2017). *Cosmetic ingredients review: An update on safety assessments*. *Journal of Cosmetic Dermatology*, 16(4), 524-531. doi:10.1111/jocd.12355

22. Kavanagh, R. M., & Egan, R. W. (2018). *Emulsifiers and stabilizers in cosmetics: Theory and practice*. *International Journal of Cosmetic Science*, 40(3), 235-247. doi:10.1111/ics.12460

23. Canet, A., & Sanz, M. (2018). *Food additives and flavorings: An overview*. *Food Chemistry*, 243, 367-380. doi:10.1016/j.foodchem.2017.10.077

24. McClements, D. J. (2018). *Food structure design for improved health*. *Current Opinion in Food Science*, 22, 62-68. doi:10.1016/j.cofs.2018.01.009

25. "Hydrogenated Castor Oil and its Derivatives" in *Chemical Engineering Journal* (2017). doi:10.1016/j.cej.2017.03.096.

26. K. H. Johnson and C. L. Davis, "Physical and Chemical Properties of Cosmetic Emulsifiers," *Cosmetic Science and Technology* (2019). doi:10.1002/cst.12425.

27. J. Smith, "Odor and Sensory Evaluation of Emulsifiers in Personal Care Products," *Journal of Sensory Studies* (2018). doi:10.1111/joss.12355.

28. A. M. Martinez and S. A. Gomez, "Solubility of Polyethylene Glycol Derivatives in Organic Solvents," *Solvent Extraction and Ion Exchange* (2019). doi:10.1080/07366299.2019.1654847.

29. Zhang, Q., & Liu, Y. (2021). "PEG-50 hydrogenated castor oil as an excipient in pharmaceutical formulations: Enhancing drug solubility and bioavailability." *Pharmaceutics*, 13(2), 145.

30. Wang, T., & Chen, X. (2020). "Formulation and efficacy of topical creams incorporating PEG-50 hydrogenated castor oil." *European Journal of Pharmaceutics and Biopharmaceutics*, 151, 57-64.

31. Ma, H., & Li, X. (2014). "Emulsification properties and stability of PEG-50 hydrogenated castor oil in cosmetic formulations." *Journal of Cosmetic Science*, 65(4), 203-215.

32. Lee, Y., & Kim, J. (2017). "Solubilization of essential oils using PEG-50 hydrogenated castor oil in cosmetic products." *International Journal of Cosmetic Science*, 39(6), 558-565.

33. Smith, A., & Green, R. (2019). "The role of PEG-50 hydrogenated castor oil in hair conditioning formulations." *Cosmetics & Toiletries*, 134(8), 45-52.

34. Patel, S., & Kumar, R. (2018). "Formulation stability and performance of PEG-50 hydrogenated castor oil in sunscreen products." *Skin Pharmacology and Physiology*, 31(4), 214-222.

35. Trotter, J. A., & Aitken, J. B**.** "Diethylene Glycol Monoethyl Ether and Related Compounds." *Journal of Chemical Education*, 83(9), 1417-1424. doi:10.1021/ed083p1417.

36. Handbook of Physical Properties of Organic Chemicals. (2007). CRC Press. doi:10.1201/9781420005903.

37. Miller, L. J., & Smith, H. L. (2020). "Food Flavorings and Fragrances: Solubility and Stability." *Journal of Food Science and Technology*, 57(3), 1285-1296. doi:10.1007/s11483-020-04970-0.

38. Kumar, A., & Patel, R. (2021). "Advances in Food Colorant Technology." *Food Chemistry*, 339, 127952. doi:10.1016/j.foodchem.2020.127952.

39. Smith, J. A., & Johnson, P. (2020). "Solvent Extraction Techniques in Food Processing." *Journal of Agricultural and Food Chemistry*, 68(4), 918-930. doi:10.1021/acs.jafc.0c00067.

40. Roberts, S., & Matthews, P. (2019). "Emulsion Stability and Rheology in Food Systems." *Food Hydrocolloids*, 90, 218-226. doi:10.1016/j.foodhyd.2018.11.013.

41. Lee, H. S., & Cho, S. H. (2020). "Innovations in Food Packaging Materials: Plasticizers and Additives." *Packaging Technology and Science*, 33(2), 77-89. doi:10.1002/pts.2531.

42. Schrenk, D., & Li, X. (2016). Production and Application of Gellan Gum. *Advances in Applied Microbiology*, 96, 133-150. doi:10.1016/bs.aambs.2016.03.002.

43. Smyth, T. J., & Li, W. (2005). Characterization and Application of High Acyl Gellan Gum. *Carbohydrate Polymers*, 59(4), 447-453. doi:10.1016/j.carbpol.2004.11.023.

44. Lai, S. L., & Teo, S. H. (2008). Properties and Applications of Low Acyl Gellan Gum. *Journal of Applied Polymer Science*, 107(4), 2611-2618. doi:10.1002/app.27415.

45. Draget, K. I., & Smidsrød, O. (2019). Alginate-Based Hydrogels for Medical and Pharmaceutical Applications. *Gels*, 5(4), 83. doi:10.3390/gels5040083.

46. Zhang, H., & Liu, W. (2020). Drying Techniques for Gellan Gum Powder Production. *Journal of Food Engineering*, 280, 109975. doi:10.1016/j.jfoodeng.2020.109975.

47. Patel, M. M., & Patel, N. M. (2012). Applications of Gellan Gum in Pharmaceutical Formulations. *Journal of Pharmaceutical Sciences*, 101(10), 3620-3634. doi:10.1002/jps.23182.

48. Zhang, J., & Li, M. (2019). Biomedical Applications of Gellan Gum: Current Trends and Future Directions. *Journal of Biomedical Materials Research*, 107(5), 1004-1014. doi:10.1002/jbm.b.34371.

49. Liu, L., & Li, X. (2016). Gellan Gum in Cosmetics: A Review. *International Journal of Cosmetic Science*, 38(6), 511-519. doi:10.1111/ics.12314.

50. Muzzarelli, R. A. A. (2021). Chitosan-Based Hydrogels: From Synthesis to Applications. *Polymers*, 13(9), 1471. doi:10.3390/polym13091471.

51. Glicksman, M. (2015). Gellan Gum in Food Industry: Applications and Benefits. *Food Technology*, 69(2), 22-29.

52. Wu, Y., & Zhang, Q. (2021). Functionalized Gellan Gum Hydrogels: Innovations and Applications. *Carbohydrate Polymers*, 273, 118631. doi:10.1016/j.carbpol.2021.118631.

53. Wang, S., & Xu, Z. (2021). Structure and Properties of Gellan Gum and Its Applications in Food Industry. *Food Chemistry*, 341, 127873. doi:10.1016/j.foodchem.2020.127873

5. MATERIALS AND METHODS

5.1.MATERIALS USED

Resveratrol was purchased from Simson Chemie (Mumbai, India). Capryol 90 was a gift sample from Gattefosse, India. Capmul MCM and Acconon S35 were obtained from Abitec Corporation. Orynophor PH50 was purchased from Oryn Healthcare. Castor Oil, Diethylene Glycol Monoethyl Ether and Tween 20 were purchased from Sisco Research Laboratories. Poloxamer 407, Sodium Chloride, Potassium Chloride, Calcium Chloride Dihydrate, Propylene Glycol, Tween 80, Hydrochloric Acid and Oleic acid were purchased from Merck. Methanol and Acetonitrile was purchased from Spectrochem. Poloxamer 188, Gellan Gum and Dialysis Membrane-60 LA390 were purchased from HiMedia. All reagents were used as received without further purification. Double Distilled Water was used in all the experiments. The experiments were carried out at 28±5 °C unless specified otherwise.

5.2.INSTRUMENTS USED

For weighing purposes, balance used was from Mettler Toledo MA155. For spectrophotometric analysis, the UV-vis spectrophotometer used was LabIndia UV-3200 Double Beam Spectrophotometer. For Droplet Size analysis and Zeta Potential determination Malvern Zetasizer was used. The FTIR used was from Thermo Fisher Scientific. For Chromatographic analysis, HPLC used was from Shimadzu Corp. Magnetic Stirrers used were Remi 2MLH. For pipetting purposes, Micropette used was Tarsons Accupipette T-1000

5.3.METHODS

5.3.1. Pre-Requisite Work

Preparation of Simulated Nasal Fluid (SNF)

A Simulated Nasal Fluid (without mucin) was prepared using KCl (0.3% w/v), NaCl (0.88% w/v) and $CaCl_2.2H_2O$ (0.06% w/v). The salts were dissolved in the order of their increasing solubility. The pH of the resulting mixture was observed using a ChemLine Digital pH Meter. The pH was adjusted to a range of 5.4 - 6.4 using 0.1N HCl.

Since RES is a BCS Class II Drug and is practically insoluble in water, Propylene Glycol (20% v/v) was added to SNF for solubilizing the drug.

Determination of λmax and Preparation of Standard Curve

10 mg RES was weighed using Mettler Toledo electronic balance. RES was taken in a 10 ml amber volumetric flask and SNF was added upto the mark to prepare the primary stock solution. 1 ml of the primary stock solution was diluted 100 times using SNF in amber volumetric flask to prepare the secondary stock solution.

The secondary stock solution was then spectrophotometrically analysed using Shimadzu UV-vis Spectrophotometer for the range 200-400 nm using SNF as reference. The spectrum data was then analysed to obtain λmax of RES.

The secondary stock solution was serially diluted to obtain concentrations of 0 µg/ml, 1 µg/ml, 2 µg/ml, 3 µg/ml, 4 µg/ml, 5 µg/ml, 7.5 µg/ml, 10 µg/ml, 15 µg/ml, 20 µg/ml and 25 µg/ml. Spectrophotometric analysis of the solutions were performed at wavelength value of λmax using SNF as reference standard. The absorbance obtained was noted and the standard curve was plotted against concentration to obtain the slope of the equation and coefficient of linearity (R^2).

Chromatographic Analysis of RES

The RP-HPLC analysis was performed using HPLC with a UV detector. The stationary phase consisted of a C-18 column and the mobile phase consisted of Acetonitrile and aqueous solution of 10 mM KH2PO4 in the ratio 60:40. The flow rate was set at 1 ml/min **[1]**.

The calibration curve was prepared by adding 10 mg RES in 10 ml methanol and dissolving in amber volumetric flask. 1 ml of the primary stock solution was diluted 100 times using Methanol in amber volumetric flask to prepare the secondary stock solution. The secondary stock solution was serially diluted to obtain concentrations of 20 μg/ml, 30 μg/ml, 40 μg/ml, 50 μg/ml and 60 μg/ml. The AUC obtained was noted and the calibration curve was plotted against AUC to obtain the slope of the equation and coefficient of linearity (R^2).

5.3.2. Preformulation Studies

Solubility Studies in Different Excipients

Maximum Solubility of RES was determined in various Oils, Surfactants and Cosurfactants. Modified Shake Flask Method was used for this process **[2]**. 500 mg of RES was added to an amber coloured vial containing 1 ml of each vehicle and shaken on a vortex mixer for 2 min. 1 ml of each vehicle was taken in an amber glass vial containing 500 mg RES. The vial was shaken on a vortex mixture for 20 min. The vials were transferred to a water bath shaker for the next 48 hours at 35 C. The mixtures were then transferred to an amber colour centrifuge tube and centrifuged at 5000 rpm for 15 min. The supernatant was then collected. The filtrate was serially diluted 1000 times using methanol and filtered using a 0.45 µm membrane filter. The resulting solution was then analysed using RP-HPLC analysis.

Preparation of Pre-Concentrate Mix (PCT)

The Oil, Surfactant and Cosurfactant were selected on the basis of their highest solubility. Oil(10-80% v/v), Surfactant(10-80% v/v) and Cosurfactant(10-80% v/v) were added in differences of 10% v/v and maximum possible ratios were obtained. The mixture was then stirred on a vortex mixture and noticed for any phase segregation after 7 days. Absence of phase separation was a confirmation to proceed with further experimentation. Table 5.3.2.1 shows all possible developed formulations.

Table 5.3.2.1: Initial ratios for optimization

Formulation	Oil	Surfactant	Co-surfactant
	(%v/v)	(%v/v)	(%v/v)
F-1	80	10	10
F-2	70	20	10
F-3	70	10	20
F-4	60	30	10
F-5	60	20	20
F-6	60	10	30
F-7	50	40	10
F-8	50	30	20
F-9	50	20	30
F-10	50	10	40

F-11	40	50	10
F-12	40	40	20
F-13	40	30	30
F-14	40	20	40
F-15	40	10	50
F-16	30	60	10
F-17	30	50	20
F-18	30	40	30
F-19	30	30	40
F-20	30	20	50
F-21	30	10	60
F-22	20	70	10
F-23	20	60	20
F-24	20	50	30
F-25	20	40	40
F-26	20	30	50
F-27	20	20	60
F-28	20	10	70
F-29	10	80	10
F-30	10	70	20
F-31	10	60	30
F-32	10	50	40
F-33	10	40	50
F-34	10	30	60
F-35	10	20	70
F-36	10	10	80

Fourier Transform Infrared (FTIR) Analysis

The FTIR analysis was performed for RES and all the excipients separately and in various combinations. RES, Oil, Surfactant, Co-surfactant, Gellan Gum, PCT (Oil+Surfactant+Co-surfactant), SEDDS (Drug+PCT), Blank (PCT+Gellan Gum) and Form (SEDDS+Gellan Gum). The combinations were made at equal weight ratio. Before analysis, the samples were Lyophilized for 4 hours to ensure complete drying. The samples were scanned from 4000 to 400 cm^{-1}.

5.3.3. Optimization Techniques

Primary Screening of developed mixtures and determination of water ratio

A modified water titration method was employed for this study. 1 ml of PCT was added to a beaker and stirred at 1,000 rpm on a magnetic stirrer. Using a burette, DDW was added dropwise to the beaker while stirring until a transparent clear/bluish solution was obtained. The amount of water was noted. The upper limit was set at 50 ml, above which the formulations were not considered fit for further stages of optimization.

Nano-Emulsification Ability and Ternary Phase Diagram

1 ml of the selected PCT was added to 50 ml DDW and mixed for 5 min on a magnetic stirrer at 1,000 rpm. The obtained emulsions were sealed and kept at 28±5°C. The emulsions were evaluated for optical clarity by visually analysing all the developed emulsions. The obtained emulsions that were visually clear were denoted as ‘clear’ while the others were denoted as ‘turbid’ **[3]**. The ternary phase diagram was plotted using Chemix School v10.0.8.

Study Design

Stat Ease Design-Expert® software (version 12.0.1.30) was employed to optimise the selected system. The independent variables were; A:Oil concentration range, B:Surfactant concentration range, C: Co-surfactant concentration range and response variables R1: Water ratio, R2: %Transmittance, R3: Max solubility, R4: Droplet size.

The optimum nano-emulsion of this study is chosen to have the minimum ratios of surfactant and co-surfactant with the maximum ratio of oil to ensure the maximum drug encapsulation. **[4]** The optimization criteria for the responses were also set to have the least droplet size and water ratio with maximum % of transmittance and drug solubility.

5.3.4. Characterization of the Selected Systems

Saturated Solubility Study

Maximum solubility of RES in each PCT was conducted as prescribed previously. Briefly, 500mg of RES was separately added to 1 ml of each PCT in amber glass vials, the mixtures were vortex mixed on orbital shaker for 10 minutes and shaken for 72 hr on a water bath shaker at 35 C. After that, the mixtures were centrifuged for 30 min at 5000 rpm and the supernatants were collected and filtered using a 0.45 μm membrane filter. The supernatant was analysed using RP-HPLC analysis **[4]**.

Spectroscopic characterization of optical clarity

The optical clarity of the developed nano-emulsions was measured using a UV-spectrophotometer. 1 ml of the selected PCT was added to 50 ml DDW and stirred for 20 min on a magnetic stirrer at 1,000 rpm. The emulsions were evaluated for optical clarity and the percentage of transmittance (%T) was measured spectrophotometrically at 638.2 nm using DDW as reference **[5]**. A glass cuvette was used for housing both the reference and sample mixtures. The obtained emulsions that were visually clear and exhibited transmittance above 90% were nominated as clear while the others were nominated as turbid.

Stability testing of prepared formulations

The selected emulsions prepared in the ratio 1:50 were stored in a 15 ml transparent graduated centrifuge tube with cap and kept at normal laboratory conditions. Optical clarity and %T was noted at predetermined intervals of Day 0, Day 7, Day 15 and Day 30. On the aforementioned day, the mixtures were shaken vigorously for 5 seconds and kept idle at least 5 min prior to the study. The %T was determined using a UV-vis Spectrophotometer at 638.2 nm using DDW as reference. Glass cuvette was used for housing both reference and sample mixtures.

5.3.5. PREPARATION OF *in-situ* GEL

A series of solutions (0.2 %w/v, 0.3 %w/v, 0.4 %w/v, 0.5 %w/v, 0.6 %w/v, 0.7 %w/v, 0.8 %w/v, 0.9 %w/v and 1.0 %w/v) were prepared by adding varying amounts of gellan gum. Water was heated to a temperature of 80±5°C and the required amount of gellan gum was added. The temperature was maintained at 80±5°C for another 15 min while being stirred on a magnetic stirrer at 1000 rpm. The solutions were left overnight at room temperature to ensure complete hydration.

Gelling capacity of *in-situ* gel

2 ml of each gellan gum solution was taken in different test tubes. SNF (0.2 ml, 0.3 ml, 0.4 ml, 0.5 ml and 0.6 ml) was added in each test tube. The mixtures were sealed using a parafilm and placed in a hot water bath maintained at 30±2°C. After 5 mins, the test tubes were tilted horizontally to inspect the fluidity of the mixture **[6]**. The gels formed, if showed adhesion to the test tube, were considered as positive response and denoted by '+', while if they showed slipping or flowing was considered as negative response and denoted by '-'.

The gels which exhibited positive response were placed again in a water bath maintained at 35±2°C. After 5 mins, the test tubes were again tilted horizontally to inspect the fluidity of the mixture. The gels formed, if showed adhesion to the test tube, were considered as positive response and denoted by '+', while if they showed slipping or flowing was considered as negative response and denoted by '-'.

Preparation of RES *in-situ* nanoemulgel

50 mg RES was added to an amber centrifuge tube containing 1 ml of each PCT. The mix was then shaken on a vortex shaker until a clear solution was obtained. The resulting mix was then transferred to an amber vial containing 9 ml of gellan gum solution placed on a magnetic stirrer and stirred at 1000 rpm for 10 min. The formulations were stored in amber vials in a refrigerator at 5±2°C **[7].**

5.3.6. Characterization Tests for *in-situ* Nanoemulgel

Droplet size, Polydispersity Index(PDI) and Zeta Potential

50 mg RES was added to an amber vial containing 1 ml of each PCT. The drug was dissolved by shaking on a vortex mixer. After the drug was completely dissolved, the drug mixture was added to a beaker containing 9 ml aqueous solution of gellan gum. The resulting mixture was stirred on a magnetic stirrer at 1,000 rpm for 5 min. 1 ml of that formulation was taken and added to a test tube containing 9 ml of MilliQ Water. The test tube was stirred on a vortex shaker for 90 seconds. The resulting emulsions were analysed for Droplet Size, PDI and Zeta Potential using a Malvern Zetasizer.

5.4.Drug Release Study of the Developed Formulations

In-vitro Drug release study

The *in-vitro* release of RES from the formulations were carried out in an orbital shaker. 1 ml of the developed formulations were placed and sealed in a HiMedia LA390 dialysis membrane **[8]**. The receptor medium had a volume of 200 ml and was composed of SNF containing 20 %v/v Propylene Glycol. The temperature was set at 35 °C during the entire study. Samples were withdrawn at 15 min, 30 min, 60 min, 120 min, 240 min, 360 min, 720 min and 1440 min, 2880 min and 5160 min.

1 ml of sample was withdrawn at each time point and replenished simultaneously with fresh receptor media. The samples were diluted and measured spectrophotometrically at 306 nm for analysing the percentage of RES released. Percentage of RES released at each time point was compared to the RES content in the administered volume.

Drug Release Mechanism

The RES release kinetics from each formulation were compared by fitting the release data to various release models. The models were compared and the one that exhibited the highest degree of correlation (R^2) was considered as the release order of that formulation **[9]**.

5.5.REFERENCES

1. Kotta, S., Mubarak Aldawsari, H., Badr-Eldin, S. M., Alhakamy, N. A., & Md, S. (2021). Coconut oil-based resveratrol nanoemulsion: Optimization using response surface methodology, stability assessment and pharmacokinetic evaluation. Food Chemistry, 357, 129721. doi:10.1016/j.foodchem.2021.12972.
2. Zhang, P.; Liu, Y.; Feng, N.; Xu, J. Preparation and evaluation of self-microemulsifying drug delivery system of oridonin. Int. J. Pharm. 2008, 355, 269–276.
3. Balakumar K, Raghavan CV, selvan NT, prasad RH, Abdu S. Self nanoemulsifying drug delivery system (SNEDDS) of Rosuvastatin calcium: Design, formulation, bioavailability and pharmacokinetic evaluation. Colloids Surfaces B Biointerfaces 2013;112:337–43. doi:10.1016/j.colsurfb.2013.08.025
4. Salem, H. F., Kharshoum, R. M., Abou-Taleb, H. A., & Naguib, D. M. (2019). Nanosized nasal emulgel of Resveratrol: preparation, optimization, in vitro evaluation and in vivo pharmacokinetic study. Drug Development and Industrial Pharmacy, 1–32. doi:10.1080/03639045.2019.164850
5. Kumar M, Misra A, Babbar AK, Mishra AK, Mishra P, Pathak K. Intranasal nanoemulsion based brain targeting drug delivery system of risperidone. Int J Accepted Manuscript Pharm. 2008;358(1–2):285–91
6. Pund, S.; Rasve, G.; Borade, G. Ex vivo permeation characteristics of venlafaxine through sheep nasal mucosa. Eur. J. Pharm. Sci. 2013, 48, 195–201.
7. Hao, J.; Zhao, J.; Zhang, S.; Tong, T.; Zhuang, Q.; Jin, K.; Chen, W.; Tang, H. Fabrication of an ionic-sensitive in situ gel loaded with resveratrol nanosuspensions intended for direct nose-to-brain delivery. Colloids Surf. B Biointerfaces 2016, 147, 376–386.
8. Aboud HM, Ali AA, El-menshawe SF, Elbary AA. Nanotransfersomes of carvedilol for intranasal delivery: formulation, characterization and in vivo evaluation. Drug Deliv 2016;23(7):2471–81. doi:10.3109/10717544.2015.1013587
9. Salem HF, Kharshoum RM, El-ela FIA, F AG, Abdellatif KRA. Evaluation and optimization of pH - responsive niosomes as a carrier for efficient treatment of breast cancer. Drug Deliv Transl Res. 2018;8(3):633–44.

6. RESULT AND DISCUSSION

6.1.PRELIMINARY WORK

6.1.1. Determination of λmax and Preparation of Standard Curve

λmax refers to the wavelength at which a substance exhibits maximum absorbance. Standard curve is a graphical representation that shows the relationship between the concentration of a substance and its absorbance measured by a spectrophotometer at a given wavelength. It depends on Beer-Lambert law:

$$A=\varepsilon \cdot c \cdot l$$

Where,

A: absorbance

ε: molar absorptivity

c: concentration

l: path length

Table shows the Absorbance data against the sample concentration (ppm) and Figure shows the graphical representation for the given data.

Table 6.1.1.1 Standard Curve of Resveratrol

Concentration	Absorbance
0	0.0002
1	0.0697
2	0.1399
3	0.2133
4	0.2781
5	0.3553
7.5	0.5202
10	0.6773
15	1.0454
20	1.3743
25	1.7439

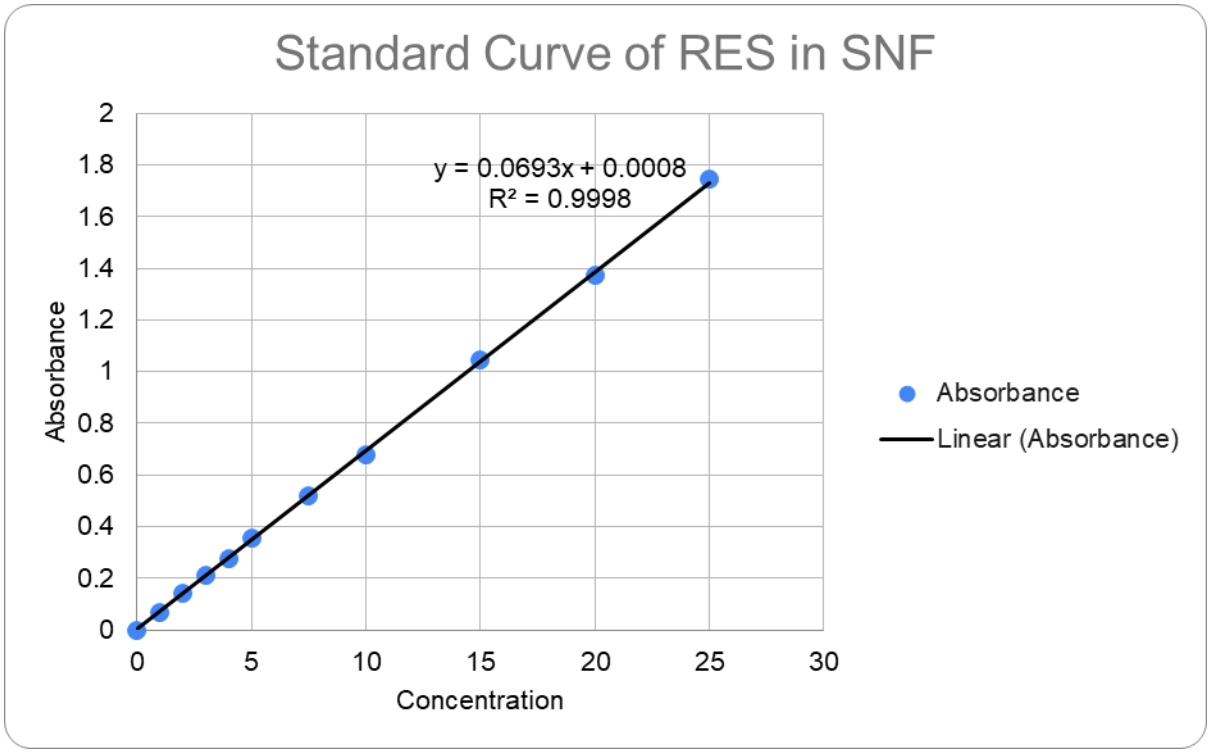

Figure 6.1.1 Standard Curve of Resveratrol

Slope	0.0693
Intercept	7.81
R^2	0.9998

6.1.2. Chromatogram of RES

HPLC is a widely used analytical technique for the separation, identification, and quantification of compounds in a mixture. HPLC is particularly useful for analysing the purity, concentration, and solubility of RES in various Excipients and Formulations.

Table 6.1.1.2 HPLC data for Calibration curve

Concentration	Area	Retention time	Peak Height
20	286840	2.422	47778
30	491451	2.426	86412
40	677620	2.426	116697
50	873311	2.43	139497
60	1048958	2.433	157990

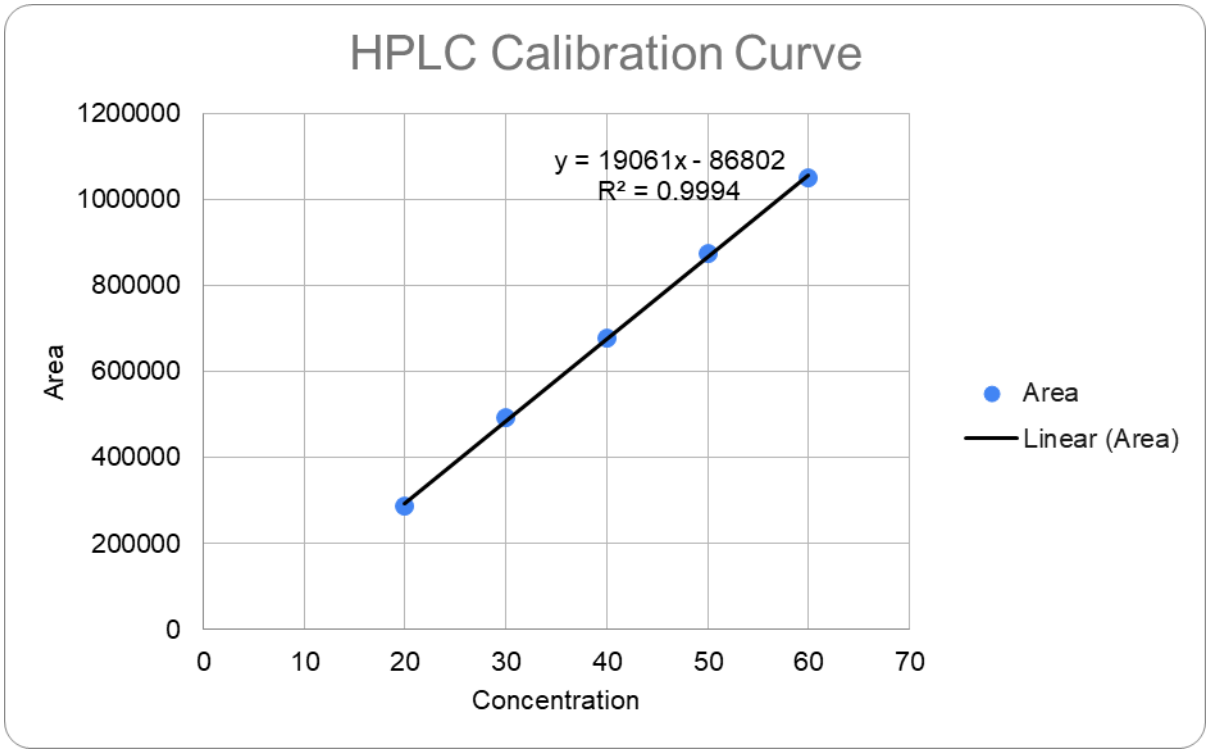

Figure 6.1.2 RES Calibration Curve

Slope	19061
Intercept	-8802
R^2	0.9994

6.2.PREFORMULATION STUDIES

6.2.1. Solubility Studies in Different Excipients

Solubility of a drug plays a big role in the screening of excipients. More the solubility, more will be the flexibility in the amount present in the developed dosage form.

Table shows the solubility data for various oils, Surfactants and Co-surfactants.

Table 6.2.1.1 RES solubility in various oils

Oils	Solubility
	(mg/ml)
Capmul MCM	20.5
Oleic Acid	4.2
Castor Oil	1.8
Capryol 90	29.9

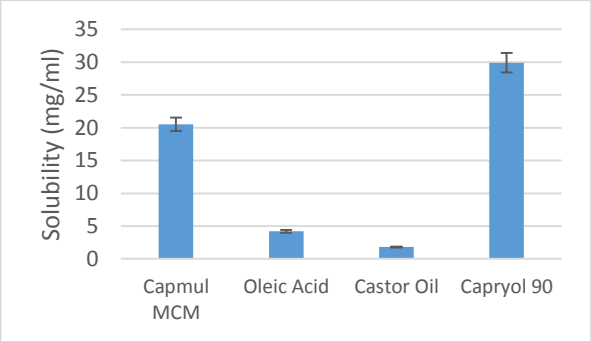

Figure 6.2.1.1 RES solubility in various oils

Table 6.2.1.2 RES solubility in various surfactants

Surfactants	Solubility
	(mg/ml)
Tween 80	94.6
Tween 20	119.2
Orynophor PH50	112.4
Labrasol	98.1
Acconon S35	59.1

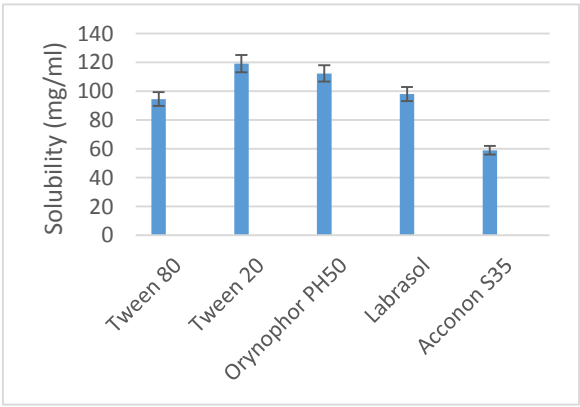

Figure 6.2.1.2 RES solubility in various surfactants

Table 6.2.1.2 RES solubility in various co-surfactants

Co-Surfactants	Solubility
	(mg/ml)
Propylene Glycol	83.9
PEG 400	132.6
Ethanol	104.4
DEGMEE	225.8

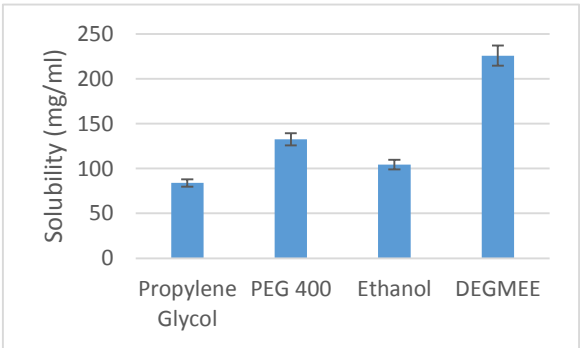

Figure 6.2.1.2 RES solubility in various co-surfactants

6.2.2. Fourier Transform Infrared (FTIR) Analysis

FTIR analysis is used to identify and characterise a chemical substance by measuring the absorption of infrared radiation by the sample. The technique provides information about molecular vibrations and functional groups within a sample, making it useful for qualitative and quantitative analysis. For development of a formulation, there should not be any chemical interaction either between the drug and excipient or between the excipients. Chemical interaction, if any, can be identified by deletion or addition of new peaks in the FTIR spectra. If it exists, the combination would be considered incompatible and would not be used in further stages of study. Figures below show the FTIR spectrum for RES, Oil, Surfactant, Co-surfactant, Gellan Gum, PCT, SEDDS, Blank and Form respectively. Upon peak analysis, some peaks showed slight shifting which could occur due to physical interaction. Although there wasn't any abrupt addition or deletion of peak. This could be due to no chemical interaction between the drug and excipients.

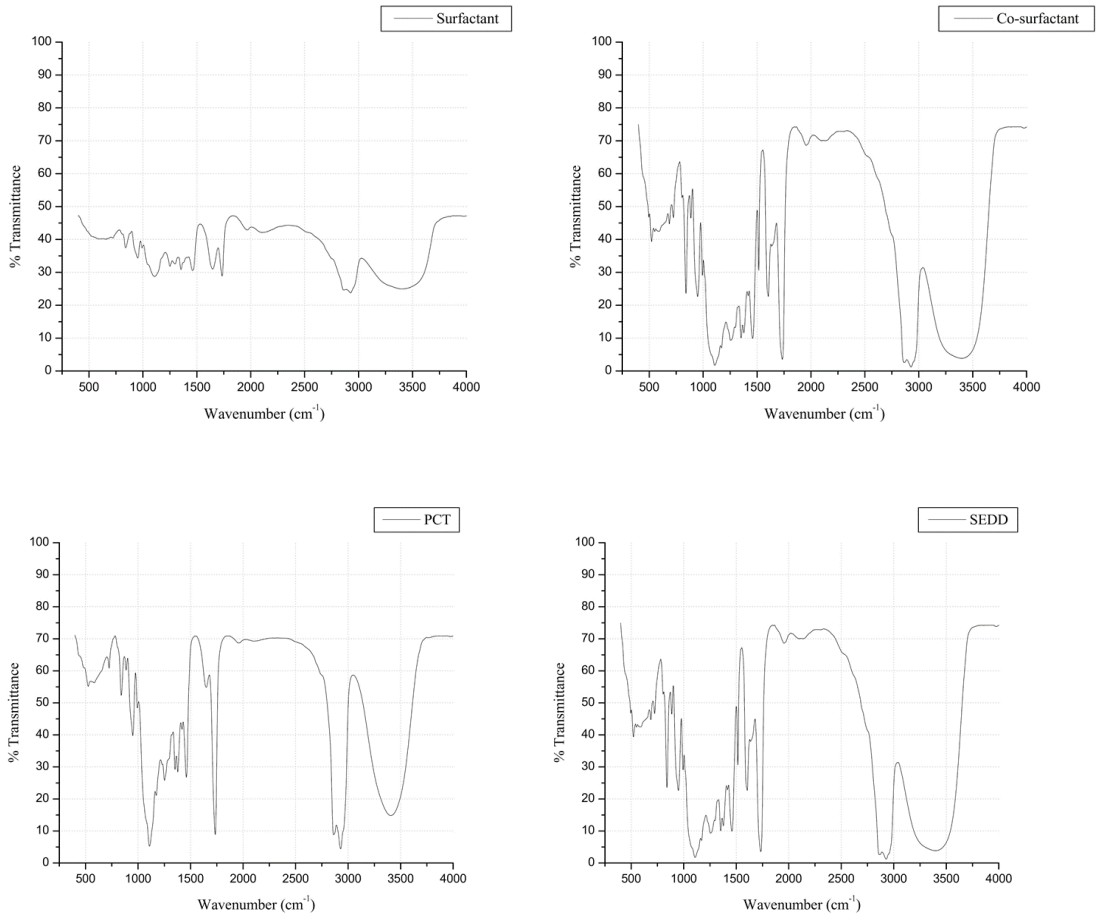

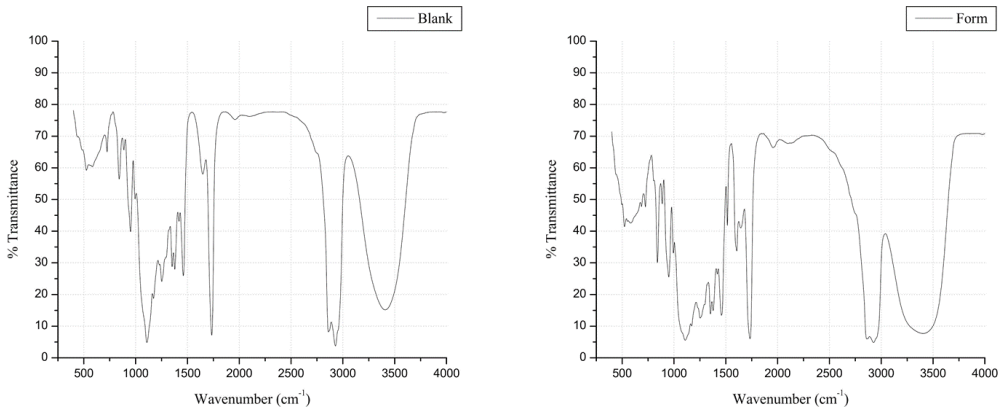

Figure 6.2.2.1 FTIR Spectra of the developed systems

Table 6.2.2.1 FTIR Spectra peaks of the developed systems

Peak Position	Group	Peak Type
3584-3700	O-H stretching	medium, sharp
3200-3550	O-H stretching	strong, broad
3100-3000	C-H stretching	weak, broad
2500-3300	O-H stretching	strong, broad
2700-3200	O-H stretching	weak, broad
1650-2000	C-H bending	weak
1735-1750	C=O stretching	strong, sharp
1625-1440	C=C stretching	weak
1250-1310	C-O stretching	strong
1200-1275	C-O stretching	strong
1163-1210	C-O stretching	strong, sharp
1085-1150	C-O stretching	strong, sharp
1087-1124	C-O stretching	strong, sharp
1050-1085	C-O stretching	strong, sharp
860-800	oop aromatic	weak, sharp
770-735	oop aromatic	weak, sharp
725-680	oop aromatic	weak, sharp
670-610	oop aromatic	weak, broad

6.3.OPTIMIZATION OF THE SYSTEMS

6.3.1. Determination of water ratio

Determining the water ratio is the first step of optimization. Table shows the amount of water needed for obtaining a clear emulsion of 1 ml PCT.

Formulation	Capryol 90	Orynophor PH50	DEGMEE	Water Ratio
	(%v/v)	(%v/v)	(%v/v)	(ml)
F-1	80	10	10	350
F-2	70	20	10	250
F-3	70	10	20	250
F-4	60	30	10	250
F-5	60	20	20	250
F-6	60	10	30	250
F-7	50	40	10	250
F-8	50	30	20	250
F-9	50	20	30	200
F-10	50	10	40	250
F-11	40	50	10	10
F-12	40	40	20	40
F-13	40	30	30	250
F-14	40	20	40	250
F-15	40	10	50	200
F-16	30	60	10	4
F-17	30	50	20	4
F-18	30	40	30	13
F-19	30	30	40	35
F-20	30	20	50	200
F-21	30	10	60	250
F-22	20	70	10	4
F-23	20	60	20	4
F-24	20	50	30	4
F-25	20	40	40	5
F-26	20	30	50	5
F-27	20	20	60	50
F-28	20	10	70	150

F-29	10	80	10	1
F-30	10	70	20	1
F-31	10	60	30	1
F-32	10	50	40	1
F-33	10	40	50	1
F-34	10	30	60	1
F-35	10	20	70	3
F-36	10	10	80	50

The increase in oil led to the use of more water for obtaining a clear/bluish transparent dispersion. Upon lowering the concentration, the surfactant: co-surfactant ratio also played a major part. The increased surfactant content used less water while higher surfactant than co-surfactant led to more water for obtaining clear/bluish dispersion.

6.3.2. Spectroscopic Characterization

For identifying a nanoemulsion, the primary criteria is the transparent/bluish colour of the emulsion. However, this is not always reliable as it is a qualitative analysis. For its quantification, spectrophotometric analysis at 632.8 nm is performed. Only the emulsions having absorbance above 90% are considered to be nanoemulsions. Table below shows the %T of the selected emulsions.

Formulation	Oil	Surfactant	Co-surfactant	%T
	(%v/v)	(%v/v)	(%v/v)	(1:50)
F-11	40	50	10	94.32
F-12	40	40	20	88.9
F-16	30	60	10	98.27
F-17	30	50	20	98.04
F-18	30	40	30	95.65
F-19	30	30	40	88.35
F-22	20	70	10	99.45
F-23	20	60	20	99.49
F-24	20	50	30	99.36
F-25	20	40	40	98.86
F-26	20	30	50	98.19
F-27	20	20	60	87.54
F-29	10	80	10	99.64
F-30	10	70	20	99.73
F-31	10	60	30	99.38
F-32	10	50	40	99.64
F-33	10	40	50	99.84
F-34	10	30	60	99.8
F-35	10	20	70	99.43
F-36	10	10	80	97.79

6.3.3. Ternary Phase Diagram

For determining the nano-emulsification ability, 36 possible ratios were developed, ranging from 10% to 80% for each surfactant, oil, and co-surfactant forming a mixture amounting to 100% of the three components. 1 ml of each mixtures were mixed on a magnetic stirrer using 50 ml double distilled water, and mixed for 5 min at 1,000 rpm using a magnetic stirrer. The obtained emulsions were evaluated for optical clarity. The ternary phase diagram for the system was plotted using CHEMIX School v12.5. Figure below shows the phase diagram for various concentrations of Capryol 90, Orynophor PH50 and DEGMEE.

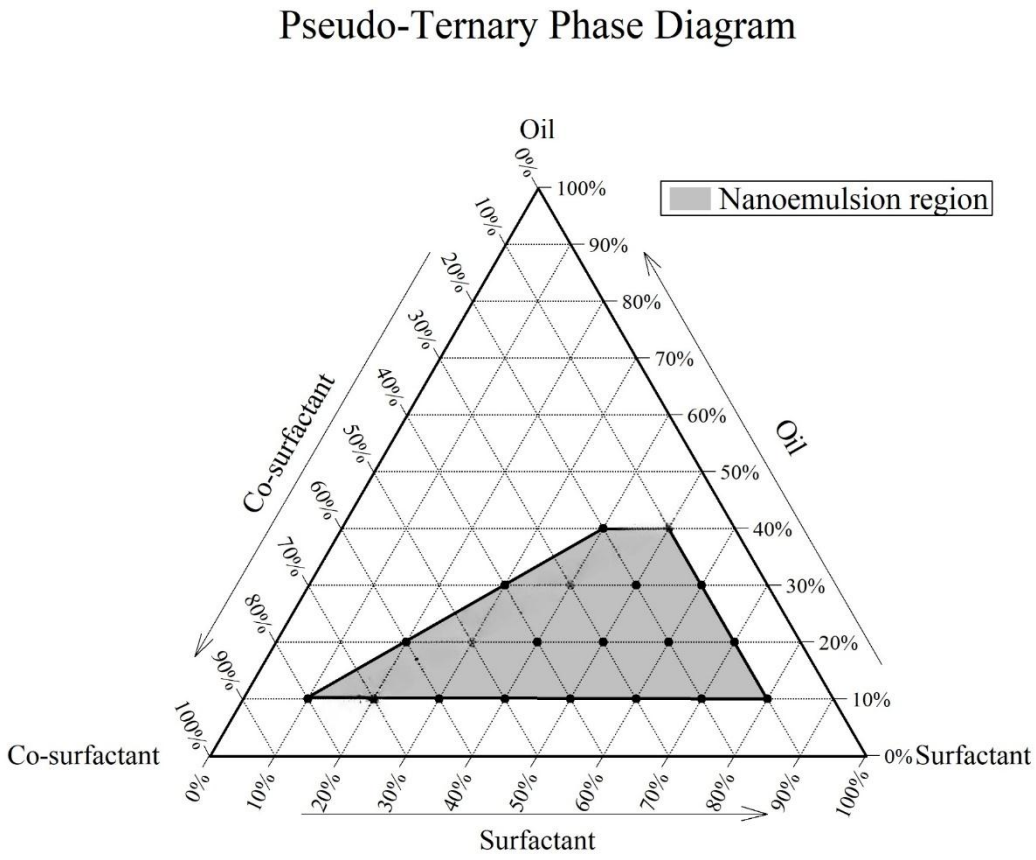

6.3.4. Saturated Solubility Study

Drug solubility is crucial for the flexibility for the concentration in the dosage form. High drug solubility ensures faster preparation of formulation and also makes it possible for creating formulations with varying concentration. Table below shows the max solubility of the selected formulations.

Table 6.4.3.1 Max Solubility of Drug in Different Mixtures

Formulation	Oil	Surfactant	Co-surfactant	Solubility
	(%v/v)	(%v/v)	(%v/v)	(mg/ml)
F-11	40	50	10	90.74
F-12	40	40	20	102.08
F-16	30	60	10	98.99
F-17	30	50	20	110.33
F-18	30	40	30	121.67
F-19	30	30	40	133.01
F-22	20	70	10	107.24
F-23	20	60	20	118.58
F-24	20	50	30	129.92
F-25	20	40	40	141.26
F-26	20	30	50	152.6
F-27	20	20	60	163.94
F-29	10	80	10	115.49
F-30	10	70	20	126.83
F-31	10	60	30	138.17
F-32	10	50	40	149.51
F-33	10	40	50	160.85
F-34	10	30	60	172.19
F-35	10	20	70	183.53
F-36	10	10	80	194.87

The saturated solubility data did not show any deviation when compared to the individual solubility of oil, surfactant and co-surfactant.

6.3.5. Stability Studies

Stability studies of formulations are essential for assessing how various products maintain their intended properties over time. For emulsions, coalescence of tiny globules may occur to form a bigger globule and cause an instability. For determination of stability, %T at various time points were noted and analysed for stability. Table below shows the %T of the developed systems at various time points.

Table 6.3.5.1 %T analyzed at different time points

Formulation	%T	%T	%T	%T
	Day 0	Day 7	Day 15	Day 30
F-11	94.32	83.62	88.49	90.08
F-12	88.9	66.09	67.92	68.83
F-16	98.27	98.08	98.2	91.1
F-17	98.04	97.24	97.59	98.65
F-18	95.65	93.71	94.32	94.49
F-19	88.35	67.51	70.53	72.61
F-22	99.45	99.81	94.25	88.32
F-23	99.49	97.91	89.7	82.31
F-24	99.36	97.82	84.22	75.67
F-25	98.86	100.28	94.5	81.7
F-26	98.19	100.27	98.45	87.51
F-27	87.54	77.64	81.92	84.15
F-29	99.64	102.8	99.97	93.86
F-30	99.73	102.51	100.17	99.41
F-31	99.38	103.12	100.19	99.55
F-32	99.64	102.43	100.14	98.77
F-33	99.84	102.84	100.08	98.8
F-34	99.8	101.63	97.92	96.57
F-35	99.43	102.29	99.25	95.24
F-36	97.79	99.57	93.15	95.17

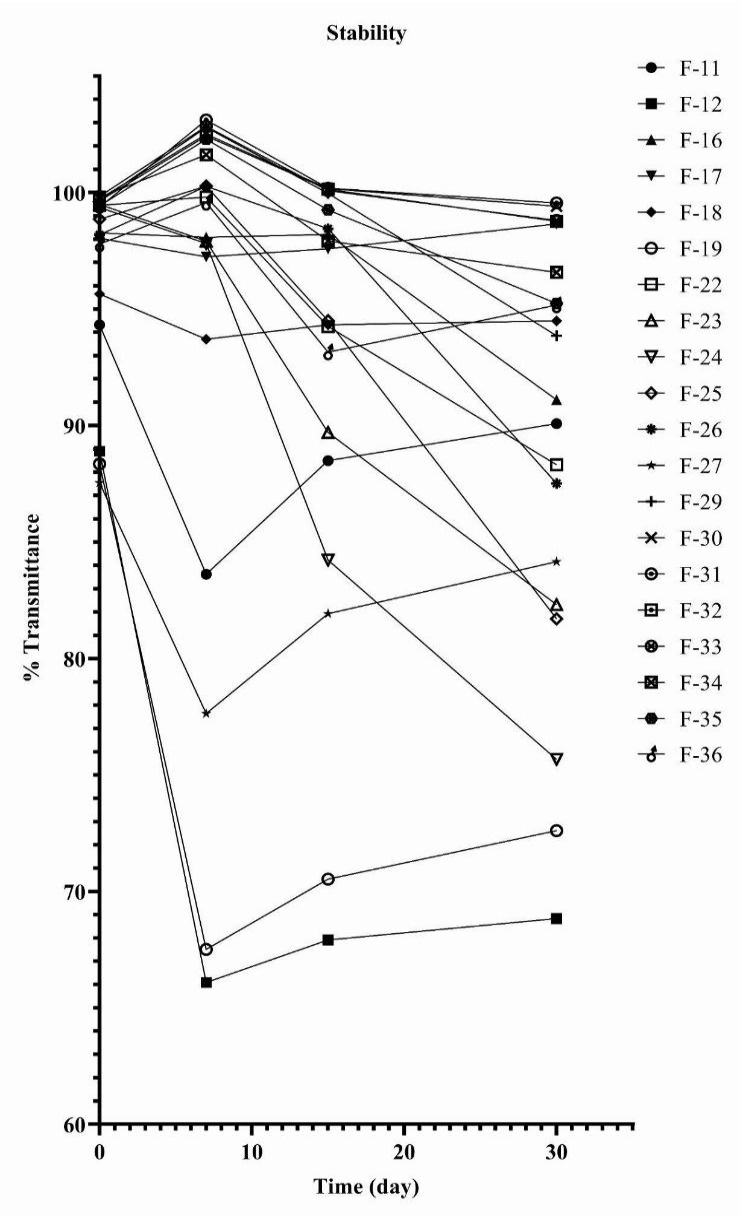

Figure 6.3.5.1 %T analyzed at different time points

The transmittance was decreased initially for systems with less ratio of Surfactant:Co-surfactant. Similar phenomena was observed with high Oil:Surfactant ratio. Conversely, it increased slightly initially for systems with more Surfactant:Co-surfactant ratio. However not much change was observed for systems with less difference in the amount of Oil, Surfactant and Co-surfactant. Figure shows the stability trend for the developed systems. Systems with high Co-surfactant showed particle deposition. This led to further increase in %T. Although this was not observed in systems with either high Oil or Surfactant.

6.4.OPTIMIZATION OF *in-situ* GELS

6.4.1. Gelling Capacity of Gellan Gum Solutions

Gelling capacity refers to the ability of a substance to convert a free flowing liquid into a gel. The intranasal in situ gelling hydrogel should stabilise the nanoemulsion in the liquid state and additionally should extend the duration of action by gelling in presence of nasal fluid at the site of absorption. Mono- and di-valent cations present in nasal fluids trigger gelation of the anionic gellan gum by binding to coordination sites and results in a structurally cross-linked three-dimensional gel matrix over the nasal mucosa.

The gelling capacity depends on the concentration of gellan gum solution and the concentration of the crosslinking ions. Since the concentration of SNF is constant, the optimization will be done on the basis of gellan gum concentration only. Table below shows the physical properties of the gellan gum solutions at 10°C, 25°C and 35°C.

Table 6.4.1.1 Gellan gum solutions at different temperatures.

Concentration (%w/v)	Temperature (10°C)	Temperature (25°C)	Temperature (35°C)
0.2	Free Flowing liquid	Free Flowing liquid	Free Flowing liquid
0.3	Free Flowing liquid	Free Flowing liquid	Free Flowing liquid
0.4	Free Flowing liquid	Free Flowing liquid	Free Flowing liquid
0.5	Free Flowing liquid	Free Flowing liquid	Free Flowing liquid
0.6	Viscous liquid	Viscous liquid	Free Flowing liquid
0.7	Semi solid gel	Viscous liquid	Viscous liquid
0.8	Semi solid gel	Semi solid gel	Viscous liquid
0.9	Semi solid gel	Semi solid gel	Semi solid gel
1.0	Semi solid gel	Semi solid gel	Semi solid gel

From the following solutions, 0.2 %w/v, 0.3 %w/v, 0.8 %w/v, 0.9 %w/v and 1.0 %w/v concentration of gellan gum solutions were not considered for next stages of optimization.

Tables below shows the gelling capacities at 25°C, 30°C and 35°C respectively. "-" indicates liquid, "+/-" indicates very soft gels and "+" indicates stable gels.

Table 6.4.1.2 Crosslinked Gellan gum at 25°C

Gel concentration	0.1 ml	0.15 ml	0.2 ml	0.25 ml	0.3 ml
0.4 %w/v	-	+/-	+/-	+	+
0.5 %w/v	-	+/-	+	+	+
0.6 %w/v	-	+/-	+	+	+

Table 6.4.1.2 Crosslinked Gellan gum at 30°C

Gel concentration	0.1 ml	0.15 ml	0.2 ml	0.25 ml	0.3 ml
0.4 %w/v	-	+/-	+/-	+	+
0.5 %w/v	-	+/-	+	+	+
0.6 %w/v	-	+/-	+	+	+

Table 6.4.1.2 Crosslinked Gellan gum at 35°C

Gel concentration	0.1 ml	0.15 ml	0.2 ml	0.25 ml	0.3 ml
0.4 %w/v	-	-	+/-	+/-	+
0.5 %w/v	-	-	+/-	+	+
0.6 %w/v	-	+/-	+/-	+	+

Based on the obtained Gelling capacity data, 0.5 %w/v solution of Gellan gum was considered as the aqueous phase for the formulations.

6.5.CHARACTERIZATION OF THE DEVELOPED SYSTEMS

6.5.1. Globule Size, PDI and Zeta Potential

The size of the globules can affect the stability, appearance, and performance of the colloidal system. In emulsions, smaller globules often lead to a more stable product, while larger globules can lead to separation over time. Since all globules are not of the same size, PDI is calculated to assess the size uniformity. A low PDI suggests uniformity in particle size, which is often desirable for consistent performance and stability. Zeta potential is a measure of the electrostatic potential at the surface of particles in a colloidal system. It indicates the degree of electrostatic repulsion between adjacent, similarly charged particles. Higher zeta potential indicates more stable dispersions, while, lower values are less stable. Table below shows the Globule Size, PDI and Zeta Potential of the developed formulations.

Formulation	Globule Size	PDI	Zeta Potential
	(nm)		(mV)
G-11	349.5	0.292	-12.9
G-16	301.4	0.293	-12.3
G-17	252.1	0.203	-17.0
G-18	192.6	0.357	-14.8
G-22	206.2	0.251	-17.21
G-23	187.3	0.193	-15.5
G-24	175.4	0.340	-14.1
G-25	166.3	0.265	-16.5
G-26	160.1	0.305	-13.9
G-27	154.4	0.339	-12.7
G-29	214.1	0.174	-17.7
G-30	198.5	0.164	-16.7
G-31	154.2	0.232	-14.5
G-32	109.2	0.341	-15.1
G-33	124.6	0.135	-15.6
G-34	99.9	0.125	-14.7
G-35	79.1	0.205	-12.3
G-36	50.2	0.342	-12.1

6.6.EXPERIMENTAL MODEL ESTIMATION

In order to obtain the optimum nanoemulgel, the effects of the studied independent variables on the dependent variables were assessed by D-optimal mixture experimental design via Design-Expert® software. The best fitted model obtained for the globule size and RES solubility was the linear model, while a special cubic model was found to be best fitted for the % transmittance. All employed models were significant at $p < 0.05$. The adjusted and the predicted coefficient of determination (R^2) were in an acceptable agreement with the obtained responses. The obtained models could be applied to circumnavigate the design space because the obtained adequate precision that measures the signal-to-noise ratio was greater than 4.

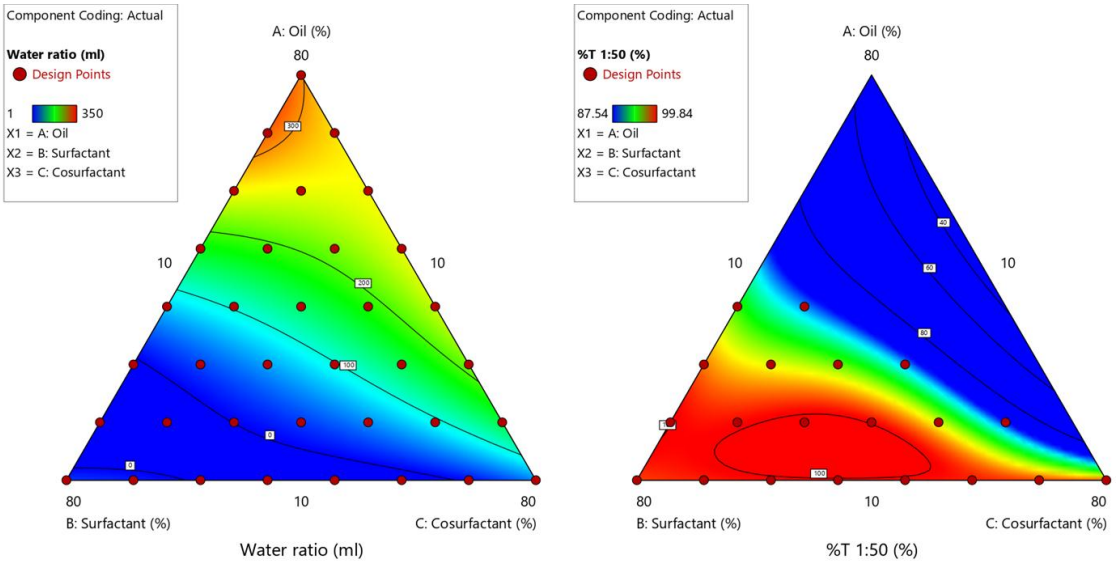

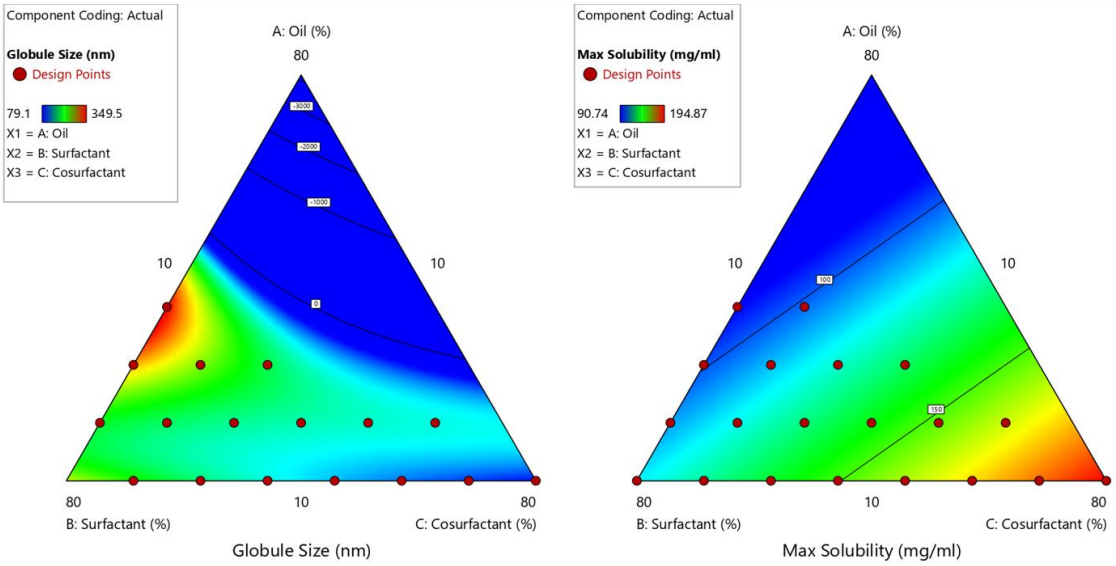

6.6.1. The optimum nanoemulgel

The goal of the optimization of the prepared formulations is to determine the levels of the independent variables to obtain an optimum product with the best characteristics. Some of the dependent variables should be minimised and others be maximised. The optimization was developed to obtain least droplet size with maximum % of transmittance and drug solubility. The optimization criteria were also set to obtain the maximum concentration of oil phase to ensure the maximum drug encapsulation and to maintain the drug in a dissolved form.

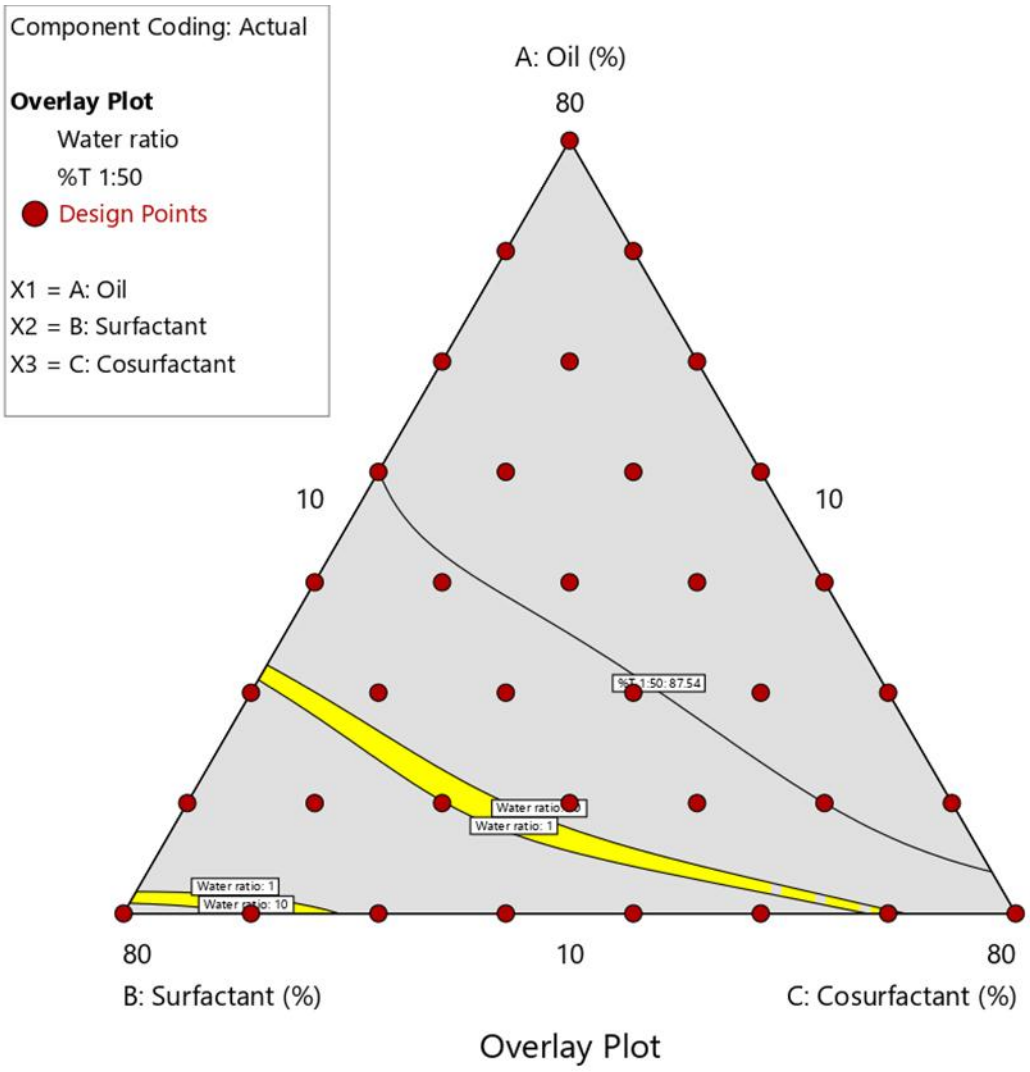

Figure 6.6.1 Desirability area of the formulations

6.7.*in-vitro* DRUG RELEASE

In-vitro drug release testing is used to evaluate the release of RES from the formulation in a simulated nasal environment. This study predicts the *in-vivo* release of RES in the nasal cavity. Table below shows the parameters for the study. The *in-vitro* release of RES from various formulations are shown in respective Tables. Figures below show the release profiles for the respective formulations at various concentrations.

Table 6.7.1 Experimental parameters for in-vitro release

Sample conc.	0.5% w/v
Media volume	200 ml
Media temperature	37 C
Sample instilled	1 ml
Shaker speed	100 rpm
Amount withdrawn	1 ml

Time (min)	G-11
0	0.00000
15	7.59019
30	12.07258
60	15.22078
120	21.64560
240	32.02713
360	39.31429
720	55.12193
1440	66.53434
2880	74.07749
5760	78.16465

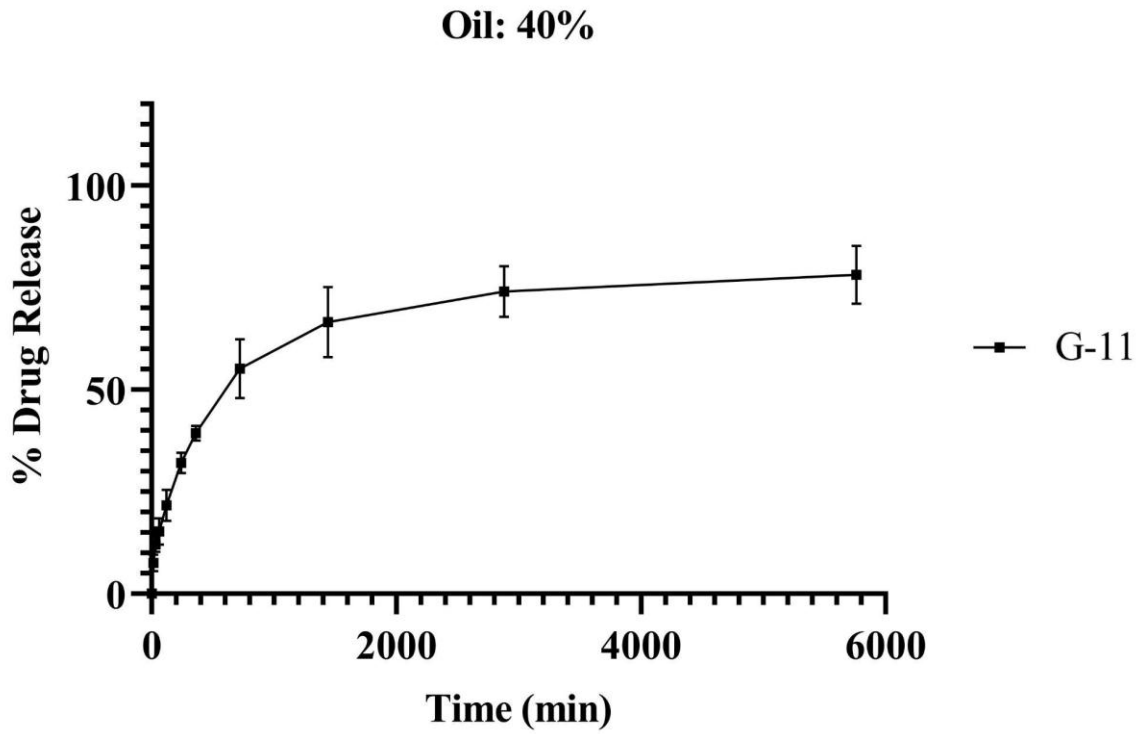

Time (min)	G-16	G-17	G-18
0	0.00000	0.00000	0.00000
15	5.19481	4.67532	6.34921
30	6.49062	6.28600	9.09380
60	9.29351	9.86710	14.85339
120	13.72641	12.91760	20.49726
240	22.76999	21.35108	33.03766
360	28.16436	26.42092	41.62872
720	42.70491	37.86479	55.08153
1440	54.11400	51.24113	62.88629
2880	60.18225	60.23896	68.96825
5760	63.48009	63.94141	71.99105

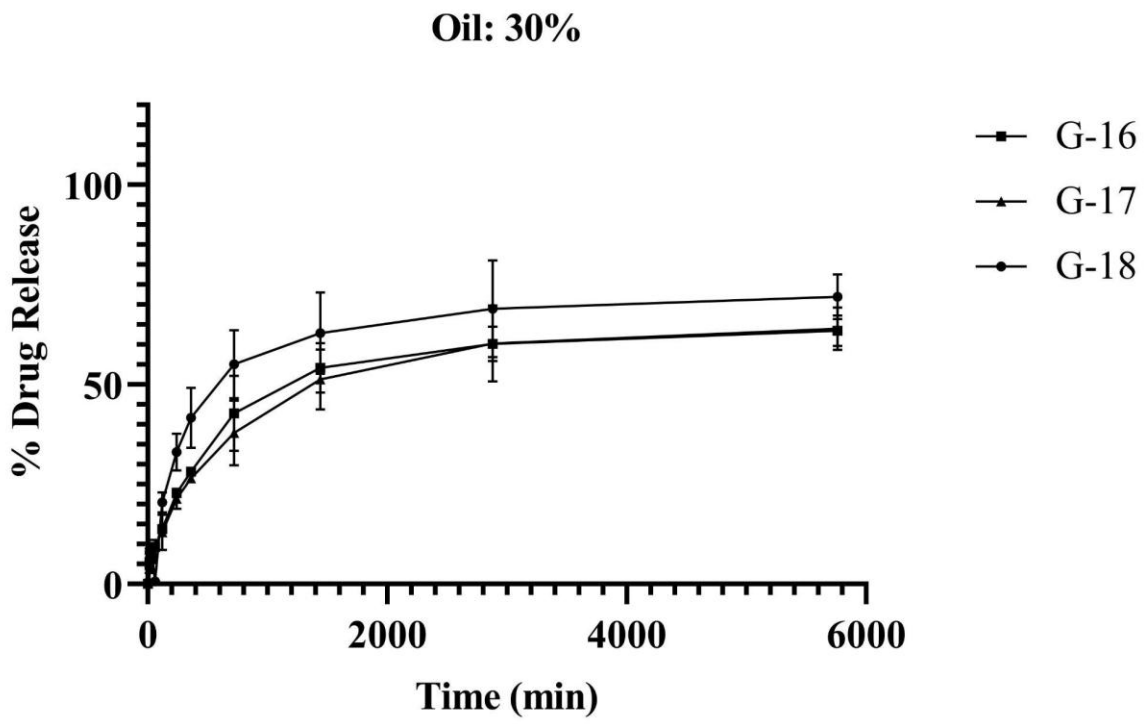

Time (min)	G-22	G-23	G-24	G-26	G-27
0	0.00000	0.00000	0.00000	0.00000	0.00000
15	7.30159	8.36941	7.67677	6.98413	5.16595
30	9.38716	12.45166	10.16825	9.29899	7.26970
60	14.54214	17.04473	15.76003	16.53146	11.75036
120	20.81934	23.65180	21.98557	22.53001	15.61833
240	29.69610	33.29293	34.18701	34.12814	26.31631
360	36.07706	39.31645	40.73463	43.09971	39.26075
720	51.20491	57.83680	62.95628	64.06335	52.29812
1440	65.68600	77.66089	83.64300	81.32121	58.44444
2880	77.87172	89.87706	102.00736	93.09380	60.43550
5760	86.68240	101.34430	111.19740	100.01703	62.31962

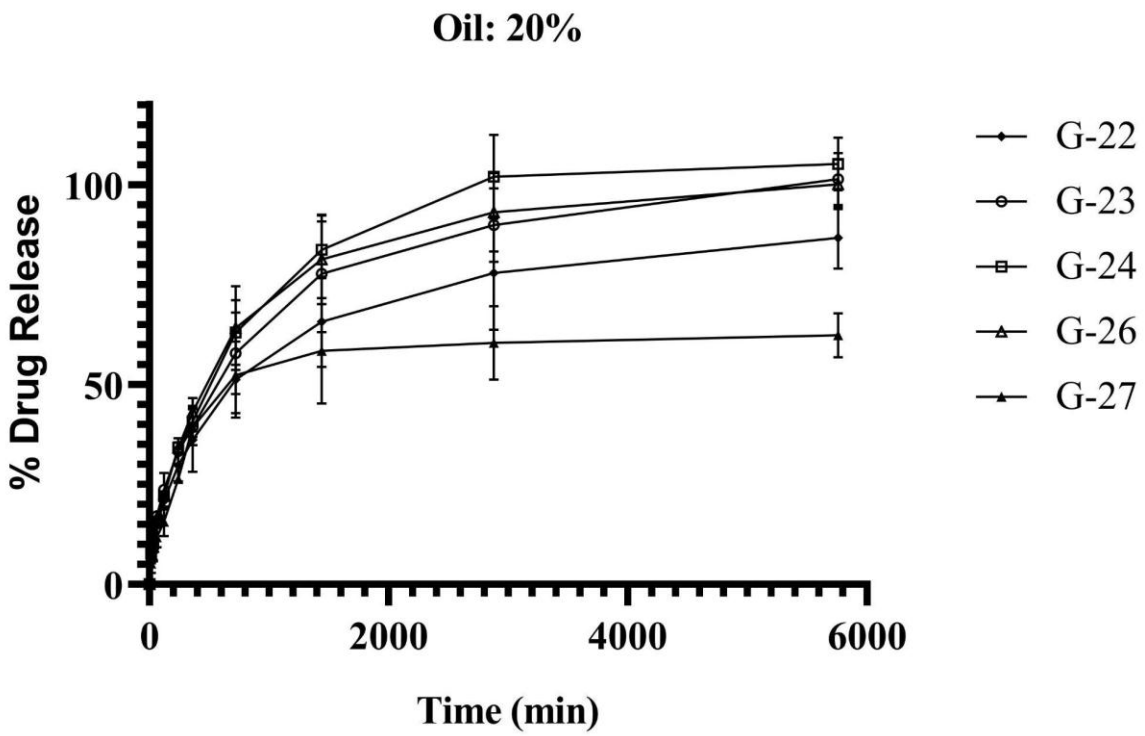

Time (min)	G-30	G-31	G-32	G-33	G-34	G-35	G-36
0	0.00000	0.00000	0.00000	0.00000	0.00000	0.00000	0.00000
15	7.44589	5.94517	6.98413	3.46320	7.90765	5.05051	5.48341
30	10.94632	9.49582	10.33795	4.69264	11.61241	8.79870	11.28283
60	16.68629	16.41183	19.22063	8.52554	16.66306	15.19177	18.95815
120	24.07085	23.30447	27.65685	11.77143	30.54098	20.66421	27.88369
240	33.19466	37.12872	37.66436	21.32482	38.28297	36.87071	42.07706
360	39.41977	45.39380	46.19163	27.80880	48.51602	43.08557	53.88759
720	57.45007	71.07302	66.65094	51.32323	74.47027	69.85007	66.16017
1440	81.37042	92.92569	89.31818	77.29221	93.10722	85.98254	68.85354
2880	98.33824	96.90606	101.3323	89.45036	100.0028	93.30505	73.55007
5760	105.2590	100.5865	106.2470	95.49134	104.3621	98.18009	75.12266

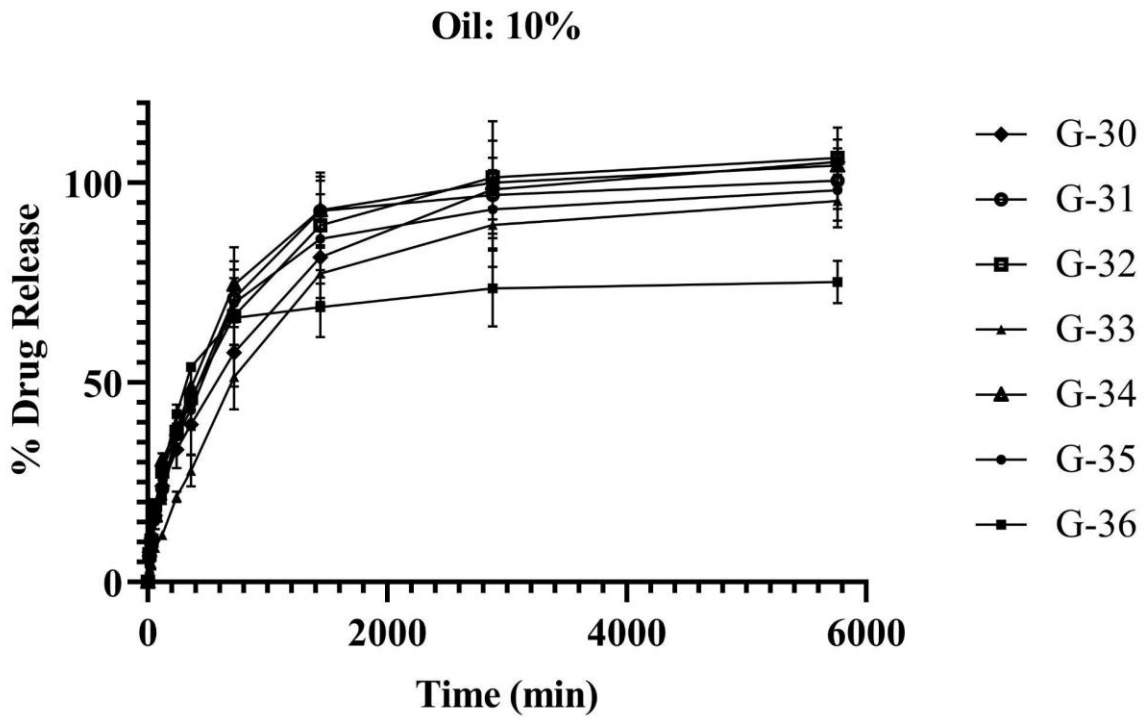

Time (min)	Suspension	Suspengel
0	0.00000	0.00000
15	3.49206	5.77201
30	5.67403	9.09091
60	9.28095	12.94574
120	13.25209	20.25397
240	16.11732	35.53492
360	19.89120	44.74459
720	27.75281	70.21876
1440	37.52915	89.12367
2880	49.74906	94.12424
5760	62.57749	98.42612

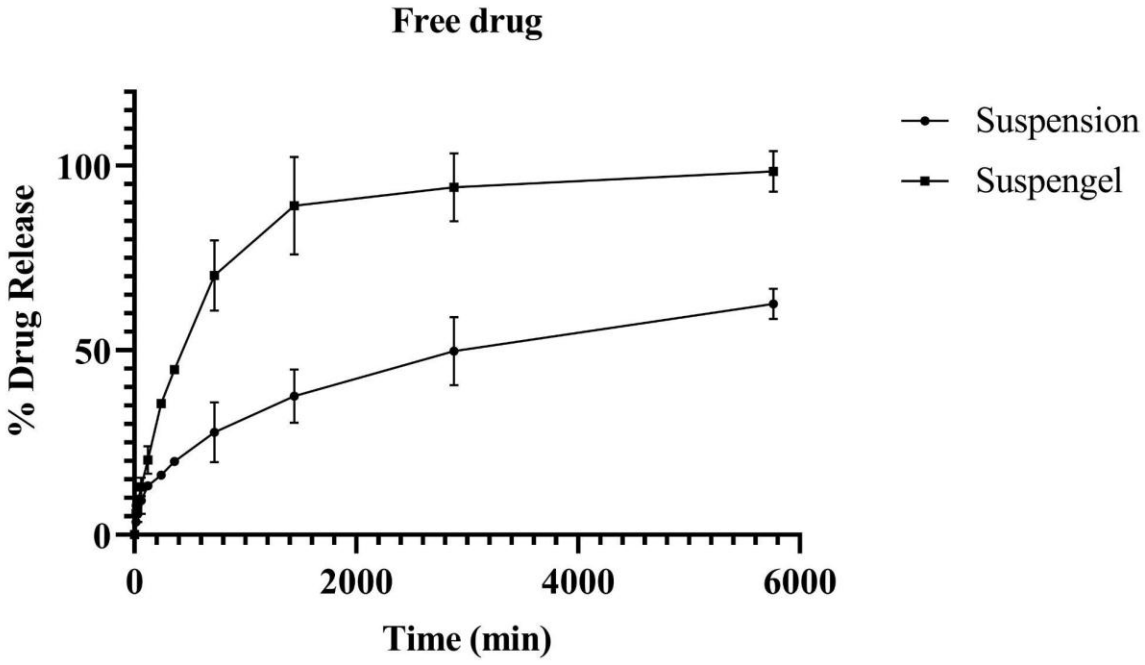

6.8.DRUG RELEASE KINETICS

Table 6.8.1 Drug Release Kinetics of the Developed Formuloations

Formulation	Zero Order	First Order	Higuchi	Korsmeyer-Peppas
	R^2	R^2	R^2	R^2
G-11	0.637145	0.774923	**0.875126**	0.594228
G-16	0.660871	0.744691	**0.888798**	0.703331
G-17	0.708332	0.794729	**0.919762**	0.717960
G-18	0.584498	0.701357	**0.834966**	0.619926
G-22	0.725975	0.905617	**0.931708**	0.639125
G-23	0.730378	0.823759	**0.933443**	0.611620
G-24	0.682123	**0.938439**	0.902711	0.649607
G-26	0.686379	0.839987	**0.906494**	0.654910
G-27	0.538810	0.607360	**0.794871**	0.662292
G-30	0.708145	0.871931	**0.918971**	0.639445
G-31	0.619548	**0.874716**	0.859204	0.666739
G-32	0.640454	**0.878530**	0.876938	0.631306
G-33	0.736999	**0.939020**	0.924627	0.811296
G-34	0.601550	**0.955967**	0.847797	0.616107
G-35	0.636935	**0.936611**	0.871242	0.688328
G-36	0.482097	0.596512	**0.746236**	0.580282
Suspension	0.848201	0.930884	**0.986848**	0.746226
Suspengel	0.626891	**0.923368**	0.863219	0.687366

The developed formulations were tested against suspension of RES and an *in-situ* gelling suspension of RES (Suspengel). All the formulations including Free Drug formulations showed highest order of linearity with First order and Higuchi Release Kinetics.

7. CONCLUSION

Several neurological diseases require therapies in which the drug must reach the brain. However, many drugs cannot be delivered due to the highly restrictive nature of BBB. Therefore, a non-invasive route along with nanotechnology remains of paramount significance for CNS delivery. The wide use of different nanoformulations has led to a wide array of techniques for improving brain targeting. In addition, naturally-derived medicinal components have the advantages of abundant resources, less side effects and improved efficacy, which can be utilized as potential drugs for the treatment of CNS diseases. The current study was focused on the formulating of a nasal nanoemulgel for the brain targeting of Resveratrol. Ion-activated *in situ* gel of Resveratrol was prepared successfully by using Gellan gum. Various nanoemulsion formulation trials were carried out to study the effect of various factors on globule size, PDI, and zeta potential of the formed nanoemulsions. The nanoemulsions were prepared with Resveratrol as model drug. Capryol 90, Orynophor PH50 and Diethylene Glycol Monoethyl Ether as Oil, Surfactant and Co-surfactant respectively. Concentrations of oil and surfactant, and Co-surfactant were selected as independent factors. Optimized Gellan gum solution was used as the continuous phase for the emulsions. The Water ratio, Drug Solubility and Globule size was found to follow a linear versus mean statistical model, the data for PDI and zeta potential, however did not fit any design model. The concentrations of Oil and ratio of Surfactant:Co-surfactant were found to significantly influence the globule size. The particle size, PDI, and zeta potential of the optimized formulation were found to be satisfactory. The concentration of components emulsions did not show any promising trend with stability. The *in-vitro* release data did not show any trend at all. The possible explanation could be due to Resveratrol being a sensitive drug to oxygen, heat, light and presence of metal ions. The presence of all the factors could contribute to relative less amount of Resveratrol in the dissolution media. The developed phytochemical-based nanoemulgel technology may provide a potential platform that could off-set the major short-comings of the conventional liquid formulations for nasal administration by virtue of its nano-sized lipid-based particles and ion-triggered gelation with natural biocompatible hydrogel polymer for the treatment of chronic CNS disorders.

8. FUTURE ASPECTS

The formulation of an *in-situ* nanoemulgel of Resveratrol is a versatile topic and require vast studies along with high precision due to the highly sensitive nature of Resveratrol. Although a lot of study has been performed, it still needs more work to establish the final formulation. As of now, the work still remains to be concluded and needs multiple studies prior to that.

- Further Opimisation of the Nanoemulgel
- Evaluation and Characterization of the developed formulations
- Real-time stability study in various conditions
- *Ex-vivo* Drug Permeation Studies
- *In-vivo* Pharmacokinetic Studies
- *In-vivo* Pharmacodynamic study using a disease model